

Novel genes and sex differences in COVID-19 severity

Raquel Cruz^{1,2,3,4,†}, Silvia Diz-de Almeida^{4,†}, Miguel López de Heredia², Inés Quintela¹, Francisco C. Ceballos⁵, Guillermo M. Lorenzo-Salazar⁷, Rafaela González-Montelongo⁷, Manuela Gago-Domínguez^{8,3}, Marta Sevilla Porras^{2,9}, Jair Antonio Tenorio Castaño^{2,9,10}, Julian Nevado^{2,9,10}, Jose María Aguado^{11,12,13,14}, Carlos Aguilar¹⁵, Sergio Aguilera-Albesa^{16,17}, Virginia Almadana¹⁸, Berta Almoguera^{19,2}, Nuria Alvarez⁶, Álvaro Andreu-Bernabeu^{20,13}, Eunat Arana-Arri^{21,22}, Celso Arango^{20,23,13}, María J. Arranz²⁴, María-Jesus Artiga²⁵, Raúl C. Baptista-Rosas^{26,27,28}, María Barreda-Sánchez^{29,30}, Moncef Belhassen-Garcia^{31,32}, Joao F. Bezerra³³, Marcos A.C. Bezerra³⁴, Lucía Boix-Palop³⁵, María Brion^{36,37}, Ramón Brugada^{38,39,37,40}, Matilde Bustos⁴¹, Enrique J. Calderón^{42,43,44}, Cristina Carbonell^{45,32}, Luis Castano^{21,46,2,47,48}, Jose E. Castelao⁴⁹, Rosa Conde-Vicente⁵⁰, M. Lourdes Cordero-Lorenzana⁵¹, Jose L. Cortes-Sanchez^{52,53}, Marta Corton^{19,2}, M. Teresa Darnaude⁵⁴, Alba De Martino-Rodríguez^{55,56}, Víctor del Campo-Pérez⁵⁷, Aranzazu Diaz de Bustamante⁵⁴, Elena Domínguez-Garrido⁵⁸, Andre D. Luchessi⁵⁹, Rocío Eiros⁶⁰, Gladys Mercedes Estigarribia Sanabria⁶¹, María Carmen Fariñas^{62,63,64}, Uxía Fernández-Robelo⁶⁵, Amanda Fernández-Rodríguez^{5,14}, Tania Fernández-Villa⁶⁶, Belén Gil-Fournier⁶⁷, Javier Gómez-Arrue^{55,56}, Beatriz González Álvarez^{55,56}, Fernan Gonzalez Bernaldo de Quirós⁶⁸, Javier González-Peñas^{20,13,23}, Juan F. Gutiérrez-Bautista⁶⁹, María José Herrero^{70,71}, Antonio Herrero-Gonzalez⁷², María A. Jimenez-Sousa^{5,14}, María Claudia Lattig^{73,74}, Anabel Liger Borja⁷⁵, Rosario Lopez-Rodriguez^{19,2}, Esther Mancebo^{76,77}, Caridad Martín-López⁷⁵, Vicente Martín^{78,43}, Oscar Martinez-Nieto^{79,74}, Iciar Martinez-Lopez^{80,81}, Michel F. Martinez-Resendez⁵², Angel Martinez-Perez⁸², Juliana F. Mazzeu^{83,84,85}, Eleuterio Merayo Macías⁸⁶, Pablo Minguez^{19,2}, Victor Moreno Cuerda^{87,88}, Vivian N. Silbiger⁵⁹, Silviene F. Oliveira^{83,89,90,91,92}, Eva Ortega-Paino²⁵, Mara Parellada^{20,23,13}, Estela Paz-Artal^{76,77,93}, Ney P.C. Santos⁹⁴, Patricia Pérez-Matute⁹⁵, Patricia Perez⁹⁶, M. Elena Pérez-Tomás²⁹, Teresa Perucho⁹⁷, Mel Lina Pinsach-Abuin^{38,37}, Ericka N. Pompa-Mera⁹⁸, Gloria L. Porras-Hurtado⁹⁹, Aurora Pujol^{100,2,101}, Soraya Ramiro León⁶⁷, Salvador Resino^{5,14}, Marianne R. Fernandes^{94,102}, Emilio Rodríguez-Ruiz^{103,3}, Fernando Rodriguez-Artalejo^{104,105,43,106}, José A. Rodriguez-Garcia¹⁰⁷, Francisco Ruiz Cabello^{69,108,109}, Javier Ruiz-Hornillos^{110,111,112}, Pablo Ryan^{113,114,115}, José Manuel Soria⁸², Juan Carlos Souto¹¹⁶, Eduardo Tamayo^{117,118}, Alvaro Tamayo-Velasco¹¹⁹, Juan Carlos Taracido-Fernandez⁷², Alejandro Teper¹²⁰, Lilian Torres-Tobar¹²¹, Miguel Urioste¹²², Juan Valencia-Ramos¹²³, Zuleima Yáñez¹²⁴, Ruth Zarate¹²⁵, Tomoko Nakanishi^{126,127,128,129,130}, Sara Pigazzini^{131,132}, Frauke Degenhardt^{133,134}, Guillaume Butler-Laporte^{135,128}, Douglas Maya-Miles^{136,137}, Luis Bujanda^{138,137}, Youssef Bouysran¹³⁹, Adriana Palom^{140,141,142}, David Ellinghaus^{143,133}, Manuel Martínez-Bueno¹⁴⁴, Selina Rolker¹⁴⁵, Sara Amitrano¹⁴⁶, Luisa Roade^{137,140,147}, Francesca Fava^{148,149,150}, Christoph D. Spinner¹⁵¹, Daniele Prati¹⁵², David Bernardo^{153,137}, Federico Garcia^{154,155}, Gilles Darcis^{156,157}, Israel Fernández-Cadenas¹⁵⁸, Jan Cato Holter^{159,160}, Jesus M. Banales^{161,137}, Robert Frithiof¹⁶², Stefano Duga^{163,164}, Rosanna Asselta^{163,164}, Alexandre C. Pereira¹⁶⁵, Manuel Romero-Gómez^{136,137}, Beatriz Nafria-Jiménez¹⁶⁶, Johannes R. Hov^{167,160,168}, Isabelle Migeotte^{169,139}, Alessandra Renieri^{148,149,150}, Anna M. Planas^{170,171}, Kerstin U. Ludwig¹⁴⁵, Maria Buti^{137,140,147}, Souad Rahmouni¹⁵⁶, Marta E. Alarcón-Riquelme^{144,172}, Eva C. Schulte^{173,174,175}, Andre Franke^{133,134}, Tom H. Karlsen^{167,160,176}, Luca Valenti^{177,178}, Hugo Zeberg^{179,180}, Brent Richards^{181,128,182}, Andrea Ganna^{132,183}, Mercè Boada^{184,185}, Itziar de Rojas^{184,185}, Agustín Ruiz^{184,185}, Pascual Sánchez-Juan¹⁸⁶, Luis Miguel Real¹⁸⁷, SCOURGE Cohort Group*, HOSTAGE Cohort Group*, GRA@CE Cohort Group*, Encarna Guillen-Navarro^{29,188,189,190}, Carmen Ayuso^{19,2}, Anna González-Neira⁶, José A. Riancho^{62,63,64}, Augusto Rojas-Martinez¹⁹¹, Carlos Flores^{7,192,193,194,†}, Pablo Lapunzina^{2,9,10,†} and Angel Carracedo^{1,2,3,4,8,†}

¹Centro Nacional de Genotipado (CEGEN), Universidade de Santiago de Compostela, 15706 Santiago de Compostela, Spain

²Centre for Biomedical Network Research on Rare Diseases (CIBERER), Instituto de Salud Carlos III, 28029 Madrid, Spain

³Instituto de Investigación Sanitaria de Santiago (IDIS), 15706 Santiago de Compostela, Spain

Received: February 15, 2022. Revised: May 16, 2022. Accepted: June 1, 2022

© The Author(s) 2022. Published by Oxford University Press.

This is an Open Access article distributed under the terms of the Creative Commons Attribution License (<https://creativecommons.org/licenses/by/4.0/>), which permits unrestricted reuse, distribution, and reproduction in any medium, provided the original work is properly cited.

- ⁴Centro Singular de Investigación en Medicina Molecular y Enfermedades Crónicas (CIMUS), Universidade de Santiago de Compostela, 15782 Santiago de Compostela, Spain
- ⁵Unidad de Infección Viral e Inmunidad, Centro Nacional de Microbiología (CNM), Instituto de Salud Carlos III (ISCIII), 28220 Madrid, Spain
- ⁶Spanish National Cancer Research Centre, Human Genotyping-CEGEN Unit, 28029 Madrid, Spain
- ⁷Genomics Division, Instituto Tecnológico y de Energías Renovables, 38600 Santa Cruz de Tenerife, Spain
- ⁸Fundación Pública Galega de Medicina Xenómica, Sistema Galego de Saúde (SERGAS), 15706 Santiago de Compostela, Spain
- ⁹Instituto de Genética Médica y Molecular (INGEMM), Hospital Universitario La Paz-IDIPAZ, 28046 Madrid, Spain
- ¹⁰ERN-ITHACA-European Reference Network
- ¹¹Unit of Infectious Diseases, Hospital Universitario 12 de Octubre, Instituto de Investigación Sanitaria Hospital 12 de Octubre (imas12), 28041 Madrid, Spain
- ¹²Spanish Network for Research in Infectious Diseases (REIPI RD16/0016/0002), Instituto de Salud Carlos III, 28029 Madrid, Spain
- ¹³School of Medicine, Universidad Complutense, 28040 Madrid, Spain
- ¹⁴Centro de Investigación Biomédica en Red de Enfermedades Infecciosas (CIBERINFEC), Instituto de Salud Carlos III, 28029 Madrid, Spain
- ¹⁵Hospital General Santa Bárbara de Soria, 42005 Soria, Spain
- ¹⁶Pediatric Neurology Unit, Department of Pediatrics, Navarra Health Service Hospital, 31008 Pamplona, Spain
- ¹⁷Navarra Health Service, NavarraBioMed Research Group, 31008 Pamplona, Spain
- ¹⁸Hospital Universitario Virgen Macarena, Neumología, 41009 Seville, Spain
- ¹⁹Department of Genetics & Genomics, Instituto de Investigación Sanitaria-Fundación Jiménez Díaz University Hospital - Universidad Autónoma de Madrid (IIS-FJD, UAM), 28040 Madrid, Spain
- ²⁰Department of Child and Adolescent Psychiatry, Institute of Psychiatry and Mental Health, Hospital General Universitario Gregorio Marañón (IiSGM), 28007 Madrid, Spain
- ²¹Biocruces Bizkaia HRI, 48903 Barakaldo, Bizkaia, Spain
- ²²Cruces University Hospital, Osakidetza, 48903 Barakaldo, Bizkaia, Spain
- ²³Centre for Biomedical Network Research on Mental Health (CIBERSAM), Instituto de Salud Carlos III, 28029 Madrid, Spain
- ²⁴Fundació Docència I Recerca Mutua Terrassa, 08221 Terrassa, Spain
- ²⁵Spanish National Cancer Research Center, CNIO Biobank, 28029 Madrid, Spain
- ²⁶Hospital General de Occidente, 45170 Zapopan, Jalisco, Mexico
- ²⁷Centro Universitario de Tonalá, Universidad de Guadalajara, 45425 Tonalá, Jalisco, Mexico
- ²⁸Centro de Investigación Multidisciplinario en Salud, Universidad de Guadalajara, 45425 Tonalá, Jalisco, Mexico
- ²⁹Instituto Murciano de Investigación Biosanitaria (IMIB-Arrixaca), 30120 Murcia, Spain
- ³⁰Universidad Católica San Antonio de Murcia (UCAM), 30120 Murcia, Spain
- ³¹Hospital Universitario de Salamanca-IBSAL, Servicio de Medicina Interna-Unidad de Enfermedades Infecciosas, 37007 Salamanca, Spain
- ³²Universidad de Salamanca, 37007 Salamanca, Spain
- ³³Escola Técnica de Saúde, Laboratório de Vigilância Molecular Aplicada, 68515-000 Pará, Brazil
- ³⁴Federal University of Pernambuco, Genetics Postgraduate Program, Recife 50670-907, PE, Brazil
- ³⁵Hospital Universitario Mutua Terrassa, 08221 Terrassa, Spain
- ³⁶Instituto de Investigación Sanitaria de Santiago (IDIS), Xenética Cardiovascular, 15706 Santiago de Compostela, Spain
- ³⁷Centre for Biomedical Network Research on Cardiovascular Diseases (CIBERCV), Instituto de Salud Carlos III, 28029 Madrid, Spain
- ³⁸Cardiovascular Genetics Center, Institut d'Investigació Biomèdica Girona (IDIBGI), 17190 Girona, Spain
- ³⁹Medical Science Department, School of Medicine, University of Girona, 17190 Girona, Spain
- ⁴⁰Hospital Josep Trueta, Cardiology Service, 17190 Girona, Spain
- ⁴¹Institute of Biomedicine of Seville (IBiS), Consejo Superior de Investigaciones Científicas (CSIC)- University of Seville- Virgen del Rocío University Hospital, 41013 Seville, Spain
- ⁴²Departamento de Medicina, Hospital Universitario Virgen del Rocío, Universidad de Sevilla, 41013 Seville, Spain
- ⁴³Centre for Biomedical Network Research on Epidemiology and Public Health (CIBERESP), Instituto de Salud Carlos III, 28029 Madrid, Spain
- ⁴⁴Instituto de Biomedicina de Sevilla, 41013 Seville, Spain
- ⁴⁵Hospital Universitario de Salamanca-IBSAL, Servicio de Medicina Interna, 37007 Salamanca, Spain
- ⁴⁶Osakidetza, Cruces University Hospital, 48903 Barakaldo, Bizkaia, Spain
- ⁴⁷Centre for Biomedical Network Research on Diabetes and Metabolic Associated Diseases (CIBERDEM), Instituto de Salud Carlos III, 28029 Madrid, Spain
- ⁴⁸University of Pais Vasco, UPV/EHU, 48903 Bizkaia, Spain
- ⁴⁹Oncology and Genetics Unit, Instituto de Investigación Sanitaria Galicia Sur, Xerencia de Xestión Integrada de Vigo-Servizo Galego de Saúde, 36312 Vigo, Spain
- ⁵⁰Hospital Universitario Río Hortega, 47012 Valladolid, Spain
- ⁵¹Servicio de Medicina intensiva, Complejo Hospitalario Universitario de A Coruña (CHUAC), Sistema Galego de Saúde (SERGAS), 15009 A Coruña, Spain
- ⁵²Tecnológico de Monterrey, 64718 Monterrey, Mexico
- ⁵³Otto von Guericke University, Department of Microgravity and Translational Regenerative Medicine, 39106 Magdeburg, Germany
- ⁵⁴Hospital Universitario Mostoles, Unidad de Genética, 28935 Madrid, Spain
- ⁵⁵Instituto Aragonés de Ciencias de la Salud (IACS), 50009 Zaragoza, Spain
- ⁵⁶Instituto Investigación Sanitaria Aragón (IIS-Aragon), 50009 Zaragoza, Spain
- ⁵⁷Preventive Medicine Department, Instituto de Investigación Sanitaria Galicia Sur, Xerencia de Xestión Integrada de Vigo-Servizo Galego de Saúde, 36312 Vigo, Spain
- ⁵⁸Unidad Diagnóstico Molecular. Fundación Rioja Salud, 26006 La Rioja, Spain
- ⁵⁹Universidade Federal do Rio Grande do Norte, Departamento de Análises Clínicas e Toxicológicas, 59012-570 Natal, Brazil
- ⁶⁰Hospital Universitario de Salamanca-IBSAL, Servicio de Cardiología, 37007 Salamanca, Spain
- ⁶¹Instituto Regional de Investigación en Salud-Universidad Nacional de Caaguazú, HH36+J3Q Caaguazú, Paraguay
- ⁶²IDIVAL, 39008 Cantabria, Spain
- ⁶³Universidad de Cantabria, 39008 Cantabria, Spain
- ⁶⁴Hospital U M Valdecilla, 39008 Cantabria, Spain
- ⁶⁵Urgencias Hospitalarias, Complejo Hospitalario Universitario de A Coruña (CHUAC), Sistema Galego de Saúde (SERGAS), 15009 A Coruña, Spain
- ⁶⁶Grupo de Investigación en Interacciones Gen-Ambiente y Salud (GIIGAS) - Instituto de Biomedicina (IBIOMED), Universidad de León, 24071 León, Spain
- ⁶⁷Hospital Universitario de Getafe, Servicio de Genética, 28905 Madrid, Spain
- ⁶⁸Ministerio de Salud Ciudad de Buenos Aires, Buenos Aires C1425EFD CABA, Argentina
- ⁶⁹Hospital Universitario Virgen de las Nieves, Servicio de Análisis Clínicos e Inmunología, 18014 Granada, Spain
- ⁷⁰IIS La Fe, Plataforma de Farmacogenética, 46026 Valencia, Spain
- ⁷¹Universidad de Valencia, Departamento de Farmacología, 46010 Valencia, Spain
- ⁷²Data Analysis Department, Instituto de Investigación Sanitaria-Fundación Jiménez Díaz University Hospital - Universidad Autónoma de Madrid (IIS-FJD, UAM), 28040 Madrid, Spain
- ⁷³Universidad de los Andes, Facultad de Ciencias, Bogotá 111711, Colombia

- ⁷⁴SIGEN Alianza Universidad de los Andes - Fundación Santa Fe de Bogotá, Bogotá 111711, Colombia
- ⁷⁵Hospital General de Segovia, Medicina Intensiva, 40002 Segovia, Spain
- ⁷⁶Hospital Universitario 12 de Octubre, Department of Immunology, 28041 Madrid, Spain
- ⁷⁷Instituto de Investigación Sanitaria Hospital 12 de Octubre (imas12), Transplant Immunology and Immunodeficiencies Group, 28041 Madrid, Spain
- ⁷⁸Instituto de Biomedicina (IBIOMED), Universidad de León, 24071 León, Spain
- ⁷⁹Fundación Santa Fe de Bogotá, Departamento Patología y Laboratorios, Bogotá 111711, Colombia
- ⁸⁰Unidad de Genética y Genómica Islas Baleares, 07120 Islas Baleares, Spain
- ⁸¹Hospital Universitario Son Espases, Unidad de Diagnóstico Molecular y Genética Clínica, 07120 Islas Baleares, Spain
- ⁸²Genomics of Complex Diseases Unit, Research Institute of Hospital de la Santa Creu i Sant Pau, IIB Sant Pau, 08041 Barcelona, Spain
- ⁸³Faculdade de Medicina, Universidade de Brasília, Brasília 70910-900, Brazil
- ⁸⁴Programa de Pós-Graduação em Ciências Médicas, Universidade de Brasília, Brasília 70910-900, Brazil
- ⁸⁵Programa de Pós-Graduação em Ciências da Saúde, Universidade de Brasília, Brasília 70910-900, Brazil
- ⁸⁶Hospital El Bierzo, Unidad Cuidados Intensivos, 24404 León, Spain
- ⁸⁷Hospital Universitario Mostoles, Medicina Interna, 28935 Madrid, Spain
- ⁸⁸Universidad Francisco de Vitoria, 28223 Madrid, Spain
- ⁸⁹Programa de Pós-Graduação em Biologia Animal, Universidade de Brasília, Brasília 70910-900, Brazil
- ⁹⁰Programa de Pós-Graduação Profissional em Ensino de Biologia, Universidade de Brasília, Brasília 70910-900, Brazil
- ⁹¹Programa de Pós-Graduação Profissional em Ensino de Biologia (UnB), Universidade de Brasília, Brasília 70910-900, Brazil
- ⁹²Programa de Pós-Graduação em Ciências Médicas, Universidade de Brasília, Brasília 70910-900, Brazil
- ⁹³Universidad Complutense de Madrid, Department of Immunology, Ophthalmology and ENT, 28040 Madrid, Spain
- ⁹⁴Universidade Federal do Pará, Núcleo de Pesquisas em Oncologia, Belém, Pará 66075-110, Brazil
- ⁹⁵Infectious Diseases, Microbiota and Metabolism Unit, Center for Biomedical Research of La Rioja (CIBIR), 26006 Logroño, Spain
- ⁹⁶Inditex, 15141 A Coruña, Spain
- ⁹⁷GENYCA, 28220 Madrid, Spain
- ⁹⁸Instituto Mexicano del Seguro Social (IMSS), Centro Médico Nacional Siglo XXI, Unidad de Investigación Médica en Enfermedades Infecciosas y Parasitarias, Mexico City 02990, Mexico
- ⁹⁹Clinica Comfamiliar Risaralda, 660003 Pereira, Colombia
- ¹⁰⁰Bellvitge Biomedical Research Institute (IDIBELL), Neurometabolic Diseases Laboratory, 08908 L'Hospitalet de Llobregat, Spain
- ¹⁰¹Catalan Institution of Research and Advanced Studies (ICREA), 08010 Barcelona, Spain
- ¹⁰²Hospital Ophir Loyola, Departamento de Ensino e Pesquisa, Belém, Pará 66063-240, Brazil
- ¹⁰³Unidad de Cuidados Intensivos, Hospital Clínico Universitario de Santiago (CHUS), Sistema Galego de Saúde (SERGAS), 15706 Santiago de Compostela, Spain
- ¹⁰⁴Department of Preventive Medicine and Public Health, School of Medicine, Universidad Autónoma de Madrid, 28049 Madrid, Spain
- ¹⁰⁵IdiPaz (Instituto de Investigación Sanitaria Hospital Universitario La Paz), 28046 Madrid, Spain
- ¹⁰⁶IMDEA-Food Institute, CEI UAM+CSIC, 28049 Madrid, Spain
- ¹⁰⁷Complejo Asistencial Universitario de León, 24071 León, Spain
- ¹⁰⁸Instituto de Investigación Biosanitaria de Granada (ibs GRANADA), 18012 Granada, Spain
- ¹⁰⁹Universidad de Granada, Departamento Bioquímica, Biología Molecular e Inmunología III, 18071 Granada, Spain
- ¹¹⁰Hospital Infanta Elena, Allergy Unit, Valdemoro, 28342 Madrid, Spain
- ¹¹¹Instituto de Investigación Sanitaria-Fundación Jiménez Díaz University Hospital - Universidad Autónoma de Madrid (IIS-FJD, UAM), 28040 Madrid, Spain
- ¹¹²Faculty of Medicine, Universidad Francisco de Vitoria, 28223 Madrid, Spain
- ¹¹³Hospital Universitario Infanta Leonor, 28031 Madrid, Spain
- ¹¹⁴Complutense University of Madrid, 28040 Madrid, Spain
- ¹¹⁵Gregorio Marañón Health Research Institute (IiSGM), 28007 Madrid, Spain
- ¹¹⁶Haemostasis and Thrombosis Unit, Hospital de la Santa Creu i Sant Pau, IIB Sant Pau, 08041 Barcelona, Spain
- ¹¹⁷Hospital Clínico Universitario de Valladolid, Servicio de Anestesiología y Reanimación, 47003 Valladolid, Spain
- ¹¹⁸Universidad de Valladolid, Departamento de Cirugía, 47005 Valladolid, Spain
- ¹¹⁹Hospital Clínico Universitario de Valladolid, Servicio de Hematología y Hemoterapia, 47003 Valladolid, Spain
- ¹²⁰Hospital de Niños Ricardo Gutiérrez, Buenos Aires C1425EFD CABA, Argentina
- ¹²¹Fundación Universitaria de Ciencias de la Salud, 113827 Bogotá, Colombia
- ¹²²Spanish National Cancer Research Centre, Familial Cancer Clinical Unit, 28029 Madrid, Spain
- ¹²³University Hospital of Burgos, 09006 Burgos, Spain
- ¹²⁴Universidad Simón Bolívar, Facultad de Ciencias de la Salud, 080002 Barranquilla, Colombia
- ¹²⁵Centro para el Desarrollo de la Investigación Científica, 1255 Asunción, Paraguay
- ¹²⁶Institute for Molecular Medicine Finland (FIMM), 00014 University of Helsinki, Finland
- ¹²⁷McGill University, Department of Human Genetics, H3A 0G4 Montréal, Québec, Canada
- ¹²⁸Lady Davis Institute, Jewish General Hospital, McGill University, H3T 1E2 Montréal, Québec, Canada
- ¹²⁹Kyoto-McGill International Collaborative School in Genomic Medicine, Graduate School of Medicine, Kyoto University, 606-8501 Kyoto, Japan
- ¹³⁰Research Fellow, Japan Society for the Promotion of Science, 102-0083 Tokyo, Japan
- ¹³¹University of Milano-Bicocca, 20126 Milano, Italy
- ¹³²Institute for Molecular Medicine Finland, University of Helsinki, 00014 Helsinki, Finland
- ¹³³Institute of Clinical Molecular Biology, Christian-Albrechts-University, 24118 Kiel, Germany
- ¹³⁴University Hospital Schleswig-Holstein, Campus Kiel, 24118 Kiel, Germany
- ¹³⁵Department of Epidemiology, Biostatistics and Occupational Health, McGill University, H3A 0G4 Montréal, Québec, Canada
- ¹³⁶Digestive Diseases Unit, Virgen del Rocío University Hospital, Institute of Biomedicine of Seville, University of Seville, 41103 Seville, Spain
- ¹³⁷Centre for Biomedical Network Research on Hepatic and Digestive Diseases (CIBEREHD), Instituto de Salud Carlos III, 28029 Madrid, Spain
- ¹³⁸Department of Liver and Gastrointestinal Diseases, Biodonostia Health Research Institute - Donostia University Hospital, University of the Basque Country (UPV/EHU), 20014 San Sebastian, Spain
- ¹³⁹Centre de Génétique Humaine, Hôpital Erasme, Université Libre de Bruxelles, 1070 Brussels, Belgium
- ¹⁴⁰Liver Unit, Department of Internal Medicine, Hospital Universitari Vall d'Hebron, Vall d'Hebron Barcelona Hospital Campus, 08035 Barcelona, Spain
- ¹⁴¹Universitat Autònoma de Barcelona, Departament de Medicina, Bellaterra, 08193 Barcelona, Spain
- ¹⁴²Vall d'Hebron Institut de Recerca (VHIR), Liver Diseases, 08035 Barcelona, Spain
- ¹⁴³Novo Nordisk Foundation Center for Protein Research, Disease Systems Biology, Faculty of Health and Medical Sciences, University of Copenhagen, DK-2200 Copenhagen, Denmark
- ¹⁴⁴GENYO, Centre for Genomics and Oncological Research: Pfizer, University of Granada, Andalusian Regional Government, 18016 Granada, Spain
- ¹⁴⁵Institute of Human Genetics, University Hospital Bonn, Medical Faculty University of Bonn, 53127 Bonn, Germany
- ¹⁴⁶Genetica Medica, Azienda Ospedaliero-Universitaria Senese, 53100 Siena, Italy

- ¹⁴⁷Universitat Autònoma de Barcelona, Departament de Medicina, Bellaterra, 08193 Barcelona, Spain
- ¹⁴⁸University of Siena, Medical Genetics, 53100 Siena, Italy
- ¹⁴⁹Azienda Ospedaliero-Universitaria Senese, Genetica Medica, 53100 Siena, Italy
- ¹⁵⁰Med Biotech Hub and Competence Center, Department of Medical Biotechnologies, University of Siena, 53100 Siena, Italy
- ¹⁵¹Technical University of Munich, School of Medicine, University Hospital rechts der Isar, Department of Internal Medicine II, 80333 Munich, Germany
- ¹⁵²Department of Transfusion Medicine and Hematology, Fondazione IRCCS Ca' Granda Ospedale Maggiore Policlinico, Università degli Studi di Milano, 20126 Milano, Italy
- ¹⁵³Mucosal Immunology Lab, Unidad de Excelencia del Instituto de Biomedicina y Genética Molecular (IBGM, Universidad de Valladolid-CSIC), 47005 Valladolid, Spain
- ¹⁵⁴Hospital Universitario Clínico San Cecilio, 18016 Granada, Spain
- ¹⁵⁵Instituto de Investigación Ibs, Granada, 18012 Granada, Spain
- ¹⁵⁶University of Liege. GIGA-Institute, B- 4000 Liege, Belgium
- ¹⁵⁷Liege University Hospital (CHU of Liege), B- 4000 Liege, Belgium
- ¹⁵⁸Biomedical Research Institute Sant Pau (IIB Sant Pau), Stroke Pharmacogenomics and Genetics Group, 08041 Barcelona, Spain
- ¹⁵⁹Oslo University Hospital, Department of Microbiology, 0424 Oslo, Norway
- ¹⁶⁰Institute of Clinical Medicine, University of Oslo, 0424 Oslo, Norway
- ¹⁶¹Department of Liver and Gastrointestinal Diseases, Biodonostia Health Research Institute - Donostia University Hospital, University of the Basque Country (UPV/EHU), Ikerbasque, 20014 San Sebastian, Spain
- ¹⁶²Department of Surgical Sciences, Anaesthesiology and Intensive Care Medicine, Uppsala University, 751 05 Uppsala, Sweden
- ¹⁶³Humanitas University, Department of Biomedical Sciences, 20089 Milan, Italy
- ¹⁶⁴IRCCS Humanitas Research Hospital, Rozzano, 20089 Milan, Italy
- ¹⁶⁵Heart Institute (InCor)/University of Sao Paulo Medical School, 05508-070 Sao Paulo, Brazil
- ¹⁶⁶Osakidetza Basque Health Service, Donostialdea Integrated Health Organisation, Clinical Biochemistry Department, 20006 San Sebastian, Spain
- ¹⁶⁷Norwegian PSC Research Center and Section of Gastroenterology, Dept Transplantation Medicine, Oslo University Hospital, 0424 Oslo, Norway
- ¹⁶⁸Research Institute of Internal Medicine, Oslo University Hospital, 0424 Oslo, Norway
- ¹⁶⁹Fonds de la Recherche Scientifique (FNRS), B - 1000 Brussels
- ¹⁷⁰Institute for Biomedical Research of Barcelona (IIBB), National Spanish Research Council (CSIC), 08028 Barcelona, Spain
- ¹⁷¹Institut d'Investigacions Biomèdiques August Pi i Sunyer (IDIBAPS), 08036 Barcelona, Spain
- ¹⁷²Institute for Environmental Medicine, Karolinska Institutet, 171 65 Solna, Sweden
- ¹⁷³Institute of Virology, Technical University Munich/Helmholtz Zentrum München, D-85764 Munich, Germany
- ¹⁷⁴Institute of Psychiatric Phenomics and Genomics, University Hospital, LMU Munich University, 80539 Munich, Germany
- ¹⁷⁵Department of Psychiatry, University Hospital, LMU Munich University, 80539 Munich, Germany
- ¹⁷⁶Research Institute of Internal Medicine, Oslo University Hospital, 0318 Oslo, Norway
- ¹⁷⁷Università degli Studi di Milano, Department of Pathophysiology and Transplantation, 20126 Milano, Italy
- ¹⁷⁸Department of Transfusion Medicine and Hematology, Precision Medicine, Fondazione IRCCS Ca' Granda Ospedale Maggiore Policlinico, 20122 Milano, Italy
- ¹⁷⁹Karolinska Institutet, Department of Neuroscience, 171 77 Stockholm, Sweden
- ¹⁸⁰Max-Planck Institute for Evolutionary Anthropology, 04103 Leipzig, Germany
- ¹⁸¹Department of Human Genetics, Epidemiology, Biostatistics and Occupational Health, McGill University, H3A 0G4 Montréal, Québec, Canada
- ¹⁸²King's College London, Department of Twin Research, London, WC2R 2LS, United Kingdom
- ¹⁸³Massachusetts General Hospital, Harvard Medical School, Boston, MA 02114, USA
- ¹⁸⁴Research Center and Memory clinic, ACE Alzheimer Center Barcelona, Universitat Internacional de Catalunya, 08028 Barcelona, Spain
- ¹⁸⁵Centre for Biomedical Network Research on Neurodegenerative Diseases (CIBERNED), Instituto de Salud Carlos III, 28029 Madrid, Spain
- ¹⁸⁶CIBER Foundation/Queen Sofia Foundation Alzheimer Center, 28031 Madrid, Spain
- ¹⁸⁷Hospital Universitario de Valme, Unidad Clínica de Enfermedades Infecciosas y Microbiología, 41014 Sevilla, Spain
- ¹⁸⁸Sección Genética Médica - Servicio de Pediatría, Hospital Clínico Universitario Virgen de la Arrixaca, Servicio Murciano de Salud, 30120 Murcia, Spain
- ¹⁸⁹Departamento Cirugía, Pediatría, Obstetricia y Ginecología, Facultad de Medicina, Universidad de Murcia (UMU), 30100 Murcia, Spain
- ¹⁹⁰Grupo Clínico Vinculado, Centre for Biomedical Network Research on Rare Diseases (CIBERER), Instituto de Salud Carlos III, 28029 Madrid, Spain
- ¹⁹¹Tecnológico de Monterrey, Escuela de Medicina y Ciencias de la Salud, 64718 Monterrey, Mexico
- ¹⁹²Research Unit, Hospital Universitario N.S. de Candelaria, 38010 Santa Cruz de Tenerife, Spain
- ¹⁹³Centre for Biomedical Network Research on Respiratory Diseases (CIBERES), Instituto de Salud Carlos III, 28029 Madrid, Spain
- ¹⁹⁴Facultad de Ciencias de la Salud, Universidad Fernando Pessoa Canarias, 35450 Las Palmas de Gran Canaria, Spain
- *To whom correspondence should be addressed at: Unidad de Investigación, Hospital Universitario Nuestra Señora de Candelaria, Carretera del Rosario s/n, 38 010 Santa Cruz de Tenerife, Spain. Tel: +34 922602938; Fax: +34 922600545; Email: cflores@ull.edu.es (Carlos Flores); Centro de Investigación Biomédica en Red de Enfermedades Raras (CIBERER), ISCIII, Paseo de la Castellana 261, Madrid 28 046, Spain. Tel: +34 917277217; Fax: +34 912071030; Email: pablo.lapunzina@salud.madrid.org (Pablo Lapunzina); Center for Research in Molecular Medicine and Chronic Diseases (CIMUS), Av. Barcelona s/n, 15 782 Santiago de Compostela (A Coruña), Spain. Tel: +34 981951490; Fax: +34 881815403; Email: angel.carracedo@usc.es (Ángel Carracedo)

[†]These authors contributed equally: Raquel Cruz, Sílvia Diz-de Almeida.

[‡]These authors contributed equally: Carlos Flores, Pablo Lapunzina, Ángel Carracedo.

Abstract

Here, we describe the results of a genome-wide study conducted in 11939 coronavirus disease 2019 (COVID-19) positive cases with an extensive clinical information that were recruited from 34 hospitals across Spain (SCOURGE consortium). In sex-disaggregated genome-wide association studies for COVID-19 hospitalization, genome-wide significance ($P < 5 \times 10^{-8}$) was crossed for variants in 3p21.31 and 21q22.11 loci only among males ($P = 1.3 \times 10^{-22}$ and $P = 8.1 \times 10^{-12}$, respectively), and for variants in 9q21.32 near TLE1 only among females ($P = 4.4 \times 10^{-8}$). In a second phase, results were combined with an independent Spanish cohort (1598 COVID-19 cases and 1068 population controls), revealing in the overall analysis two novel risk loci in 9p13.3 and 19q13.12, with fine-mapping prioritized variants functionally associated with AQP3 ($P = 2.7 \times 10^{-8}$) and ARHGAP33 ($P = 1.3 \times 10^{-8}$), respectively. The meta-analysis of both phases with four European studies stratified by sex from the Host Genetics Initiative (HGI) confirmed the association of the 3p21.31 and 21q22.11 loci predominantly in males and replicated a recently reported variant in 11p13 (ELF5, $P = 4.1 \times 10^{-8}$). Six of the COVID-19 HGI discovered loci were replicated and an HGI-based genetic risk score predicted the severity strata in SCOURGE. We also found more SNP-heritability and larger heritability differences by age (<60 or ≥ 60 years) among males than among females. Parallel genome-wide screening of inbreeding depression in SCOURGE also showed an effect of homozygosity in COVID-19 hospitalization and severity and this effect was stronger among older males. In summary, new candidate genes for COVID-19 severity and evidence supporting genetic disparities among sexes are provided.

Introduction

Coronavirus disease 2019 (COVID-19)—caused by the severe acute respiratory syndrome coronavirus 2 (SARS-CoV-2)—develops with wide clinical variability, ranging from asymptomatic infection to a life-threatening condition (1). Advanced age and the presence of comorbidities are well-known major risk factors of COVID-19 severity (2,3). In addition, male sex is another risk factor associated with COVID-19 severity, regardless of comorbidities (4).

International genetic studies based on genome-wide association studies (GWAS) and/or comparative genome sequencing analyses have been conducted to identify genetic variants associated with COVID-19 severity (5,6). These studies have revealed the role of genes of the type-I interferon (IFN) signaling pathway as key players underlying disease severity (7–9). Besides, they have also identified other potential loci previously linked to lung function, respiratory diseases and autoimmunity (9). Regarding COVID-19 severity in males, sex-disaggregated genetic analyses have received limited attention despite the importance of sex disparities in clinical severity (10). Early studies suggested immune deficits presumably because of pre-existing neutralizing autoantibodies against type-I IFN in older male patients (11).

The effects of autozygosity, measured as the change of the mean value of a complex trait because of inbreeding, have been useful to identify alternative genetic risk explanations and effects that traditionally are not captured by GWAS (12). By analyzing the contribution of the inbreeding depression (ID) through the lens of the runs of homozygosity (ROH: genomic tracts where homozygous markers occur in an uninterrupted sequence), it is possible to assess the importance of directional dominance or overdominance in the genetic architecture of complex traits (13). Even though this is a relatively modern approach, different studies have shown the importance of homozygosity in a large range of complex phenotypes, including anthropometric, cardiometabolic and mental traits (14–16).

Through diverse nested sub-studies, the Spanish Coalition to Unlock Research on Host Genetics on COVID-19 (SCOURGE) consortium was launched in May 2020 aiming to find biomarkers of evolution and prognosis that can have an immediate impact on clinical management and therapeutic decisions in SARS-CoV-2 infections. This consortium has recruited patients from hospitals across Spain and Latin America in close collaboration with the STOP-Coronavirus initiative (<https://www.scourage-covid.org>). Here, we describe the results of the first SCOURGE genome-wide studies of COVID-19 conducted in patients recruited in Spain. This dataset has not been used in any previous GWAS of COVID-19 that has been published to date. To the best of our knowledge, this is the first time that the impact of homozygosity is considered in COVID-19 studies, serving as a complement to the traditional

GWAS to assess both the additive and dominant components of the genetic architecture of COVID-19 severity. Likewise, the ID analysis could also help to explain the strong effect of age in COVID-19 severity.

Results

Discovery phase

In the SCOURGE study, 11 939 COVID-19 positive cases were recruited from 34 centers (Supplementary Material, Table S1) between March and December 2020. All diagnosed cases were classified in a five-level severity scale (Table 1). Two untested Spanish sample collections were used as general population controls in some analyses: 3437 samples from the Spanish DNA biobank (<https://www.bancoadn.org>) and 2506 samples from the GR@CE consortium (17). The discovery phase samples were genotyped with the Axiom Spain Biobank Array (Thermo Fisher Scientific). Details of quality control (QC), ancestry inference and imputation are shown in the Materials and Methods section. Individuals with inferred European ancestry were used for association testing. After post-imputation filtering, 15 045 individuals (9371 COVID-19 positive cases and 5674 population controls) and 8 933 154 genetic markers remained in the SCOURGE European study (discovery). Clinical and demographic characteristics of European patients from SCOURGE included in the analysis are shown in Table 2. Population controls were 46.3% females with a mean age of 55.5 years (standard deviation, SD = 16.2) and 53.7% males, with a mean age of 51 years (SD = 13.04).

The discovery phase of the GWAS was carried out with infection susceptibility and three severity outcomes (hospitalization, severe illness and critical illness), which were tested using three different control definitions (see Supplementary Material, Table S2).

- A1 analysis: COVID-19 positive not satisfying the case condition and control samples from the general population (COVID-19 untested).
- A2 analysis: control samples from the general population.
- C analysis: COVID-19 positive not satisfying the case condition.

The GWAS was carried on by fitting logistic mixed regression models adjusting for age, sex and the first 10 principal components (PCs; see Materials and Methods). Summary statistics can be accessed from <https://github.com/CIBERER/Scourage-COVID19>. The SCOURGE Board of Directors has agreed to aggregate the GWAS summaries with those from the COVID-19 Host Genetics Initiative (HGI) in the data freeze 7 that has not been used for any published article to date. Supplementary Material, Table S3 shows the independent significant associated loci for hospitalization, severity, critical illness and infection susceptibility risk, for global and sex-stratified analysis in the SCOURGE dataset. However, considering the

Table 1. Five-level severity scale used to classify SCOURGE patients

Level	Clinical findings
Severity 0 (asymptomatic)	Asymptomatic
Severity 1 (mild)	With symptoms, but without pulmonary infiltrates or need of oxygen therapy
Severity 2 (moderate)	With pulmonary infiltrates affecting <50% of the lungs or need of supplemental oxygen therapy
Severity 3 (severe)	Hospitalized with any of the following criteria: <ul style="list-style-type: none"> • PaO₂ < 65 mmHg or SaO₂ < 90% • PaO₂/FiO₂ < 300 • SaO₂/FiO₂ < 440 • Dyspnea • Respiratory frequency ≥ 22 bpm • Infiltrates affecting > 50% of the lungs
Severity 4 (critical)	Admission to the ICU or need of mechanical ventilation (invasive or non-invasive)

Note: PaO₂, partial pressure of oxygen in arterial blood; SaO₂, saturation of oxygen in arterial blood; FiO₂, fraction of inspired oxygen.

Table 2. Baseline characteristics of European patients from SCOURGE included in the analysis

Variable	Global N = 9371	Males N = 4343	Females N = 5028
Age—mean years (SD)	62.6 (17.9)	64.3 (16.3)	61.1 (19.1)
Severity—N (%)			
0—asymptomatic	582 (6.6)	161 (3.9)	421 (8.9)
1—mild	2689 (30.3)	748 (18.2)	1941 (40.8)
2—intermediate	2099 (23.6)	1093 (26.5)	1006 (21.1)
3—severe	2379 (26.8)	1300 (31.6)	1079 (22.7)
4—critical illness	1128 (12.7)	817 (19.8)	311 (6.5)
Hospitalization—N (%)	5966 (63.8)	3436 (79.3)	2530 (50.5)
Severe COVID-19—N (%)	3507 (39.2)	2117 (51.2)	1390 (28.9)
Critical illness—N (%)	1128 (12.6)	817 (19.8)	311 (6.5)
Comorbidities—N (%)			
Vascular/endocrinological	4099 (43.7)	2207 (50.8)	1892 (37.6)
Cardiac	1057 (11.3)	634 (14.6)	423 (8.4)
Nervous	773 (8.3)	341 (7.9)	432 (8.6)
Digestive	264 (2.8)	153 (3.5)	111 (2.2)
Onco-hematological	647 (6.9)	411 (9.5)	236 (4.7)
Respiratory	905 (9.7)	565 (13.0)	340 (6.8)

overlap between the findings for these analyses, only the main results for the A1 analysis are presented.

All analyses support the association of two known loci, i.e. 3p21.31 and 21q22.11. However, other suggestive associations were also found (Fig. 1 and Supplementary Material, Fig. S1). Strikingly, the leading signals found in the global (sex-aggregated) analysis were genome-wide significant in the analyses among males but not among females. Association in 3p21.31 was also found in the C analyses (rs10490770, $P = 3.8 \times 10^{-12}$) and once again, association was genome-wide significant only among males (males: $P = 3.9 \times 10^{-9}$, females: $P = 4.6 \times 10^{-5}$). However, the leading variant of 9q21.32 (near TLE1 gene) reached genome-wide significance among females only (similarly, in the C analysis for females, rs140152223, $P = 2.11 \times 10^{-6}$). Several variants (rs17763742 near LZTFL1, rs2834164 in IFNAR2 and rs1826292621 near TLE1) showed a significant difference in effect sizes (SNP*sex interaction $P < 0.0031$, adjusted probability for 16 comparisons) linked not only to hospitalization, but also to critical illness and infection risk. The A2 and C analyses did not reveal any additional significant loci

(Supplementary Material, Fig. S2). Although fine-mapping studies in 3p21.31 and 21q22.11 have led to gene and variant prioritization within these loci (Supplementary Material, Fig. S3), a Bayesian fine-mapping on the 9q21.32 did not allow to prioritize variants by their role as expression quantitative trait loci (eQTLs) or anticipate the function (Fig. 2). To assess if a higher prevalence of comorbidities in males may underlie these differential findings, we performed an additional C analysis in which the presence of comorbidities was tested for association within hospitalized patients. No significant association was found in either males or females (Supplementary Material, Fig. S4). Further explorations of the genetic associations with comorbidities are presented in the Supplementary Note.

This GWAS phase was also performed disaggregated by age (<60/≥60 years old), and by age and sex simultaneously. Differences in effect sizes between both age groups were tested for the SNPs shown in the Supplementary Material, Table S3, in global and sex-specific analysis (Supplementary Material, Table S4). Significant findings were only found in the subgroup of males with <60 years

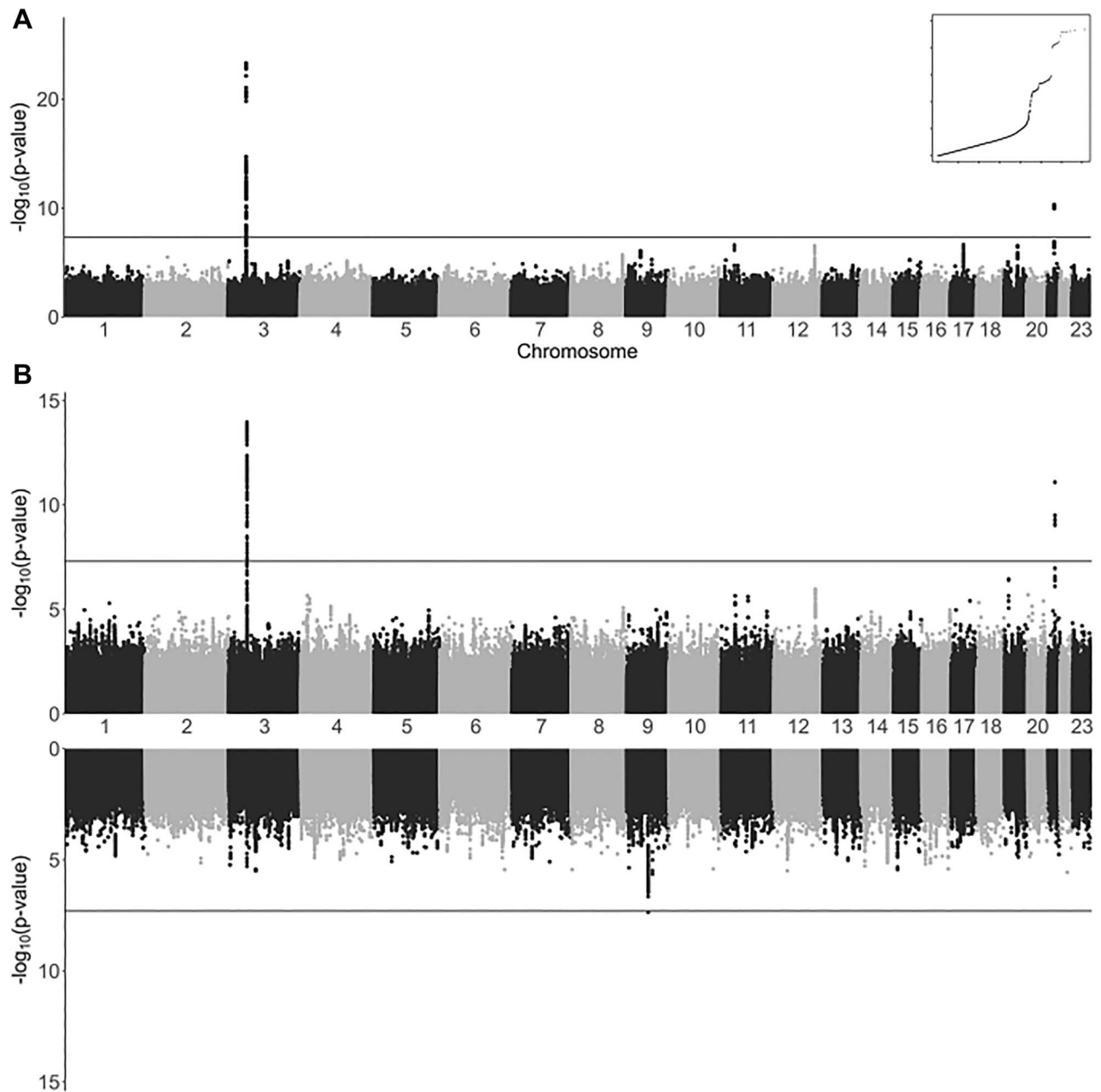


Figure 1. Association results of SCOURGE for global and sex-disaggregated A1 hospitalization analysis. (A) Manhattan plot of results from global analysis. A quantile–quantile plot of the global analysis is also shown as an inset. (B) Miami plot of results from sex-disaggregated analyses (top: males and bottom: females).

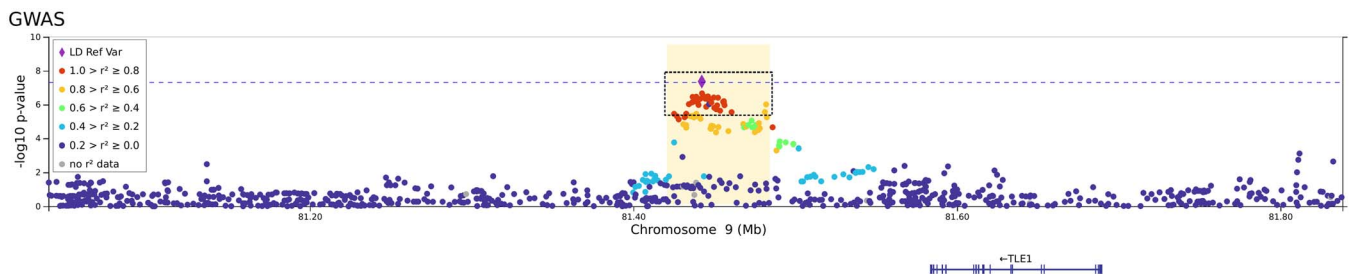


Figure 2. Regional plot of a novel association at 9q21.32 found among females from the SCOURGE study. The x axis reflects the chromosomal position, and the y axis the $-\log(\text{P-value})$. The sentinel variant is indicated by a diamond and all other variants are colour coded by their degree of LD with the sentinel variant in Europeans. Credible set for this signal is shown within a dashed square. The horizontal dotted blue line corresponds to the threshold for genome-wide significance ($P = 5 \times 10^{-8}$).

old. This was also found in the C analysis for hospitalization where association in 3p21.31 was significant only in males <60 years old ($P = 3.32 \times 10^{-9}$). Differences in effect size (significant age-interaction) were significant at 3p21.31 for severity and critical illness, and suggestive in hospitalization.

Lookup of previously found COVID-19 host risk factors in the SCOURGE study

Known significant loci for COVID-19 severity in 3p21.31 (near *SLC6A20* and *LZTFL1*) and 21q22.11 (in *IFNAR2*) were clearly replicated at genome-wide significance in this study, specifically for risk of infection, hospitalization and severity. Three other loci, in 9q34.2 (in *ABO*), 12q24.13 (in *OAS1*) and 19p13.2 (near *RAVER1* and *TYK2*), did not reach the genome-wide significance threshold but they were significant after correcting for the 390 tests performed in a lookup (13 SNPs and 30 analyses, significance threshold $P < 1.3 \times 10^{-4}$). In agreement with previous results, *ABO* was mainly associated with the risk of infection. However, other loci as those in 3q12.3 (near *RPL24*) and 19p13.3 (near *DPP9*), previously found associated with COVID-19 severity, were not replicated in the SCOURGE Europeans. The complete list of results for the list of COVID-19 HGI significant loci (9) is shown in Figure 3 and in the Supplementary Material, Table S5. Figure 3 also reinforces the clear sex differences found in this study.

Genetic risk score and the COVID-19 severity scale

We developed a genetic risk score (GRS) combining the 13 leading variants associated with infection risk, hospitalization or severity in the meta-analysis performed by the COVID-19 HGI (9). This GRS predicted the severity scale in SCOURGE but supporting the differentiation in three classes: (i) controls/asymptomatic/mild cases; (ii) moderate and severe cases and (iii) critical cases. (Supplementary Material, Fig. S5). Simultaneously disaggregating by age (<60/≥60 years old) and sex, we identify the three severity classes in the subgroup of males with <60 years old, supporting the importance of this group in the overall findings (Supplementary Material, Fig. S5). Details of this analysis can be found in Supplementary Note.

Second study phase and meta-analysis with the discovery

Results for hospitalization risk were meta-analysed with a second Spanish cohort, the CNIO study (see Materials and Methods). This study was filtered following the same QC and imputation procedures. The final dataset of the CNIO study included 2446 European individuals (1378 COVID-19 positive cases and 1068 population controls) and 8895 721 markers.

Table 3 shows the results that were genome-wide significant either in global or sex-stratified meta-analysis with SCOURGE. Besides the widely replicated loci at 3p21.31 and 21q22.11, three additional signals

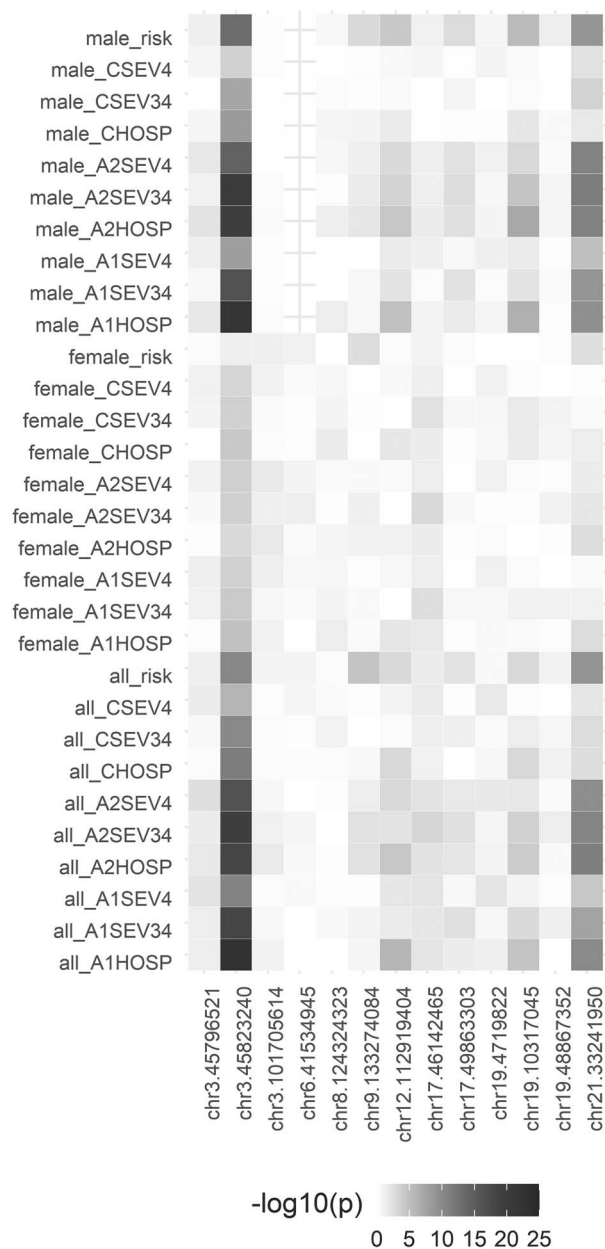


Figure 3. Lookup of previously found COVID-19 host risk factors in the SCOURGE study. Heatmap illustrating the results in all analyses performed in this study (rows) for the 13 leading variants in the COVID-19 HGI study (columns). Each box illustrates the top associated variant within the focal region. The color (gray to dark red) indicates the strength (significance level) of the association in SCOURGE. Note: In three cases (chr12: 112919388, chr19: 4719431 and chr21: 33242905), the imputed variants did not pass QC filters in SCOURGE and they were replaced by the nearest QC-ed imputed variant (chr12:112919404, chr19:4719822 and chr21:33241950, respectively).

were found: chr9:33426577:A:G (intergenic to *AQP7* and *AQP3*), chr17:45422978:G:C (intronic to *ARHGAP27*) and chr19:35687796:G:A (intergenic to *UPK1A* and *ZBTB32*). Bayesian fine-mapping around chr17:45422978:G:C failed to prioritize a credible set of variants, hindering functional links of the locus. Functional assessments of the prioritized variants by the Bayesian fine-mapping analysis in the other two regions supported that they

Table 3. Genome-wide significant variants in global or sex-stratified meta-analysis between the SCOURGE and CNIO studies

SNP	chr:position	EA	NEA	Meta-ALL			Meta-males			Meta-females			Nearest gene
				beta	SE	P-value	beta	SE	P-value	beta	SE	P-value	
rs115679256	3:45587795	G	A	0.43	0.08	1.1E-08	0.48	0.10	2.3E-06	0.40	0.11	2.9E-04	LIMD1
rs17763742	3:45805277	A	G	0.60	0.05	4.1E-29	0.74	0.07	3.3E-25	0.43	0.08	4.5E-08	LZTFL1
rs35477280	3:45932600	G	A	0.39	0.05	1.4E-17	0.48	0.06	6.3E-15	0.28	0.07	1.6E-05	FYCO1
rs4443214	3:46136372	T	C	0.25	0.04	9.0E-09	0.26	0.06	1.4E-05	0.26	0.06	4.4E-05	XCR1
rs115102354	3:46180545	A	G	0.41	0.07	1.6E-08	0.52	0.10	2.1E-07	0.32	0.10	2.0E-03	CCR3
rs10813976	9:33426577	A	G	0.18	0.03	2.7E-08	0.16	0.04	2.5E-04	0.19	0.05	3.5E-05	AQP3
rs1230082	17:45422978	C	G	0.16	0.03	2.1E-08	0.17	0.04	2.8E-05	-0.15	0.04	2.5E-04	ARHGAP27
rs77127536	19:35687796	G	A	-0.22	0.04	1.3E-08	-0.25	0.05	2.1E-06	-0.19	0.05	4.3E-04	UPK1A/ZBTB32
rs17860169	21:33240996	A	G	0.19	0.03	2.3E-11	0.27	0.04	1.4E-11	0.12	0.04	3.7E-03	IFNAR2

Note: Representative SNPs were selected using the clump function of PLINK 1.9 (clumping parameters $r^2 = 0.5$, $P_{val} = 5 \times 10^{-8}$ and $P_{val2} = 0.05$). EA, effect allele; NEA, non-effect allele; beta, effect coefficient; SE, standard error.

Table 4. Results of European meta-analysis for hospitalization risk

SNP	chr:position	EA	NEA	Meta-all			Meta-males			Meta-females			Nearest gene
				beta	SE	P-value	beta	SE	P-value	beta	SE	P-value	
rs115679256	3:45587795	G	A	0.37	0.06	1.3E-08	0.41	0.08	5.6E-07	0.36	0.09	1.6E-04	LIMD1
rs13078854	3:45820440	G	A	0.53	0.04	6.7E-34	0.64	0.05	2.7E-33	0.38	0.06	1.0E-09	LZTFL1
rs41289622	3:45973053	T	G	0.36	0.04	3.6E-21	0.44	0.05	3.4E-20	0.27	0.05	7.2E-07	FYCO1
rs115102354	3:46180545	A	G	0.40	0.06	8.9E-12	0.48	0.07	6.8E-11	0.26	0.08	1.8E-03	XCR1
rs61882275	11:34482745	G	A	-0.12	0.02	1.0E-06	-0.17	0.03	4.1E-08	-0.08	0.03	1.3E-02	ELF5
rs4767028	12:112921383	A	G	-0.16	0.02	1.6E-10	-0.19	0.03	2.5E-09	-0.11	0.04	8.7E-04	OAS1
rs12609134	19:35687796	G	A	-0.19	0.03	2.3E-08	-0.22	0.04	9.5E-08	-0.13	0.05	6.0E-03	UPK1A/ZBTB32
rs17860169	21:33240996	A	G	0.18	0.03	3.9E-12	0.21	0.03	1.6E-10	0.15	0.04	2.9E-05	IFNAR2

Note: Summary statistics of both phases (SCOURGE and CNIO) were meta-analysed with four additional sex-disaggregated European studies from the COVID-19 HGI consortium. EA, effect allele; NEA, non-effect allele; beta, effect coefficient; SE, standard error.

were eQTLs of the AQP3 and ARGAP33 genes, including whole blood and lung tissues (Fig. 4).

These variants were also associated with the three severity groups previously outlined in SCOURGE by the GRS under a multinomial model (Supplementary Material, Table S6).

Meta-analysis in independent European studies

Hospitalization risk was meta-analysed with other European studies combining both Spanish cohorts (SCOURGE and CNIO) with other four sex-disaggregated studies from the COVID-19 HGI consortium, namely: BelCOVID, GenCOVID, Hostage-Spain and Hostage-Italy (Table 4). Once again, the most outstanding significant loci were found at 3p21.31 and 21q22.11 (in global and male-specific analyses), and three additional loci reached genome-wide significance in the meta-analysis of males: chr12:11292383:A:G (in OAS1), chr19:35687796:G:A (intergenic to UPK1A and ZBTB32) and chr11:34482745:G:A (in ELF5). The 3p21.31 variants reached genome-wide significance in females, although at significantly lower level than in males despite the similar sample sizes ($Z = 3.33$, $P = 5 \times 10^{-4}$).

Significance of two interesting loci revealed in the Spanish studies was reduced in the meta-analysis with other European studies, although still showed suggestive associations: that of 9q21.32 near TLE1 previously found only in females (female meta-analysis $P = 5.4 \times 10^{-7}$),

and that of 9p13.3 near AQP3 (global meta-analysis, $P = 1.23 \times 10^{-7}$).

Heritability of COVID-19 hospitalization

In the hospitalization risk analysis, we found that common variants (minor allele frequency, MAF > 1%) explain 27.1% (95% confidence interval, CI: 19.0–35.3%) of heritability on the observed scale (corresponding to 13.1% [95%CI: 9.2–17.0%] on the liability scale, assuming a prevalence of 0.5%; Fig. 5). We observed less heritability among females than males (2.9% [95%CI: 0.00–10.6%] in females and 17.0% [95%CI: 9.2–24.9%] in males on the liability scale). In agreement with observations suggesting an accumulation of non-genetic risk factors with age, especially among males (11,18), we observed larger heritability differences by age groups among males (40.2% [95%CI: 22.8–57.5%] in <60 years versus 17.6% [95%CI: 0.00–38.0%] in ≥60 years on the liability scale) than among females (9.1% [0.00–31.3%] in <60 years versus 13.7% [0.00–29.6%] in ≥60 years on the liability scale).

ID and COVID-19 outcomes

ROH calling was performed in the European QC-ed genotyped dataset. Inbreeding depression analyses are described in Materials and Methods section and Supplemental Note.

The median genomic inbreeding coefficient, F_{ROH} , for the entire SCOURGE study was 0.0048 (IQR = 0.004). No

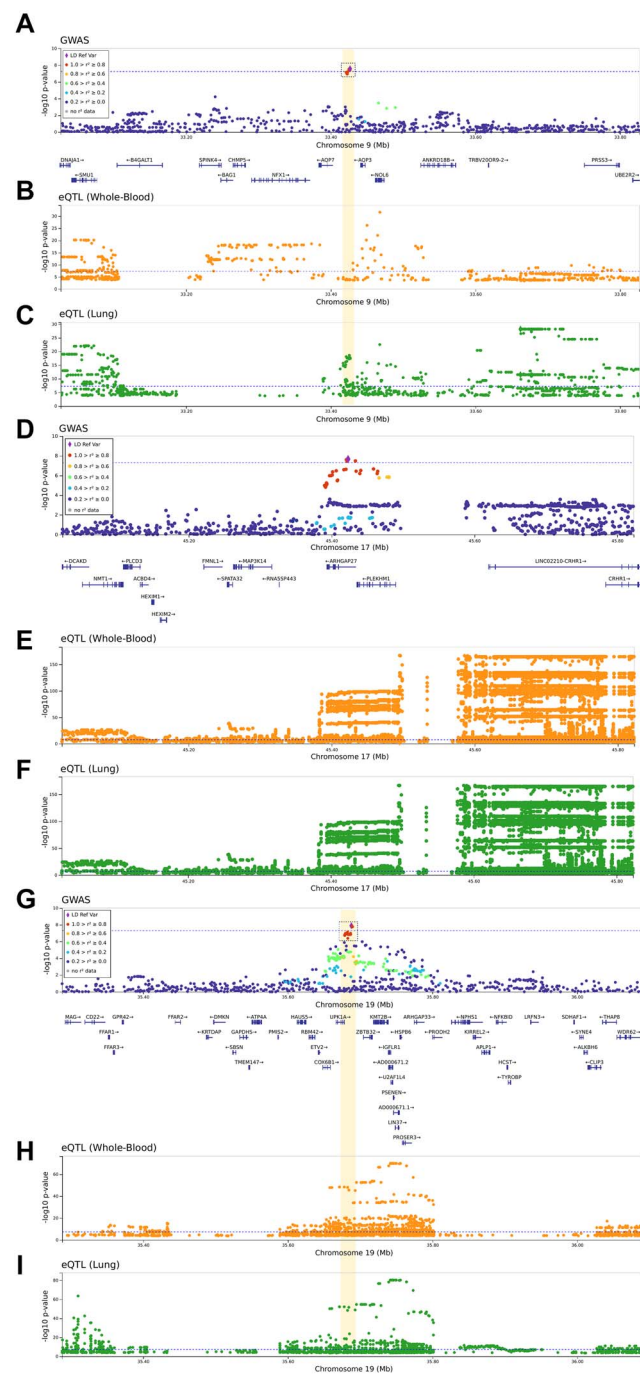


Figure 4. Regional plots of novel association signals found from the meta-analysis between the SCOURGE and CNIO studies. Regional plots of novel association signals found in 9p13.3 (A–C), 17q21.31 (D–F) and 19q13.12 (G–I). The x axes reflect the chromosomal position, and the y axes the $-\log(P\text{-value})$ of the SCOURGE-CNIO meta-analysis. On A, D and G the sentinel variant is indicated by a diamond and all other variants are color coded by their degree of LD with the sentinel variant in Europeans. Whenever a concise set of variants was prioritized, a credible set is shown within a dashed square. The horizontal dotted blue line corresponds to the threshold for genome-wide significance ($P = 5 \times 10^{-8}$). In the rest of panels, the x axes reflect the chromosomal position, and the y axes the $-\log(P\text{-value})$ resulting from the eQTL analyses in whole blood (B, E and H) and in the lung (C, F and I) whenever a significant finding is available from GTEx v8.

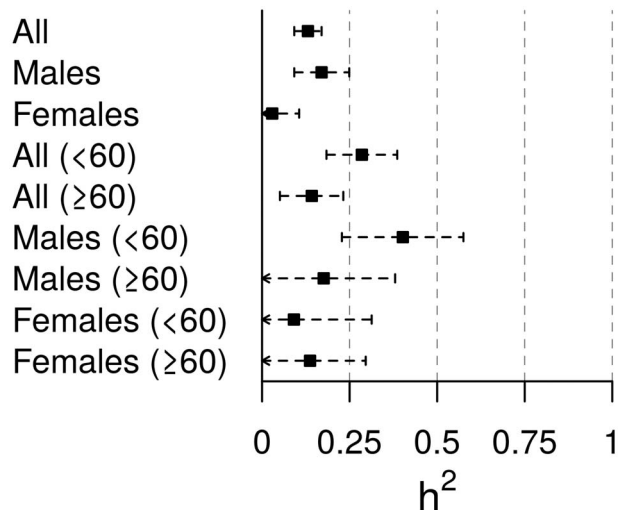


Figure 5. Forest plot of the SNP-heritability estimates for the COVID-19 hospitalization risk analysis on the liability scale.

differences were detected between males ($F_{\text{ROH}} = 0.004$, $\text{IQR} = 0.0035$) and females ($F_{\text{ROH}} = 0.0056$, $\text{IQR} = 0.0038$), or between younger and older individuals (F_{ROH} individuals < 60 years old = 0.004, $\text{IQR} = 0.0035$; F_{ROH} individuals ≥ 60 years old = 0.0052, $\text{IQR} = 0.0047$, respectively; [Supplementary Material, Fig. S6](#)). Regarding the ID in COVID-19 outcomes, we detected a positive association of the F_{ROH} in COVID-19 hospitalization risk ([Fig. 6](#)), severity risk and risk for critical illness ([Supplementary Material, Table S7](#)). Our results showed that the hospitalization odds for COVID-19 patients with an $F_{\text{ROH}} = 0.0039$ were 380% higher than individuals with $F_{\text{ROH}} = 0$. No effect of the genomic relationship matrix (F_{GRM}) was found.

To assess whether ID in COVID-19 hospitalization in SCOURGE was different between sexes, we first tested the interaction between F_{ROH} and biological sex. F_{ROH} , sex and the interaction of both ($F_{\text{ROH}}:\text{Sex}$) were significant ($F_{\text{ROH}} = 4.7 \times 10^{-3}$, $\text{Sex} = 1.0 \times 10^{-112}$, $F_{\text{ROH}}:\text{Sex} = 1.2 \times 10^{-3}$). This interaction was significant when comparing the hospitalized COVID-19 patients with different controls (A2 and C analyses, see [Supplementary Material, Table S8](#)). This interaction was also found significant with severity, but not with critical illness ([Supplementary Material, Table S8](#)). In sex-disaggregated analyses, we observed a sex-specific effect of inbreeding. F_{ROH} was significant in hospitalized males but not in females ([Fig. 6](#) and [Supplementary Material, Table S8](#)). This sex-specific effect was also observed with severity and for critical illness ([Supplementary Material, Table S8](#)). We then assessed whether ID in COVID-19 hospitalization was different by age. We detected a significant interaction between age and F_{ROH} for the three outcomes considered (hospitalization, severity and critical illness) ([Supplementary Material, Table S9](#)). After disaggregating SCOURGE by sex and age (< 60 , ≥ 60), we found that the ID for hospitalization and severity were significant mainly in older males ([Fig. 6](#) and [Supplementary Material, Table S9](#)). We detected significant ID

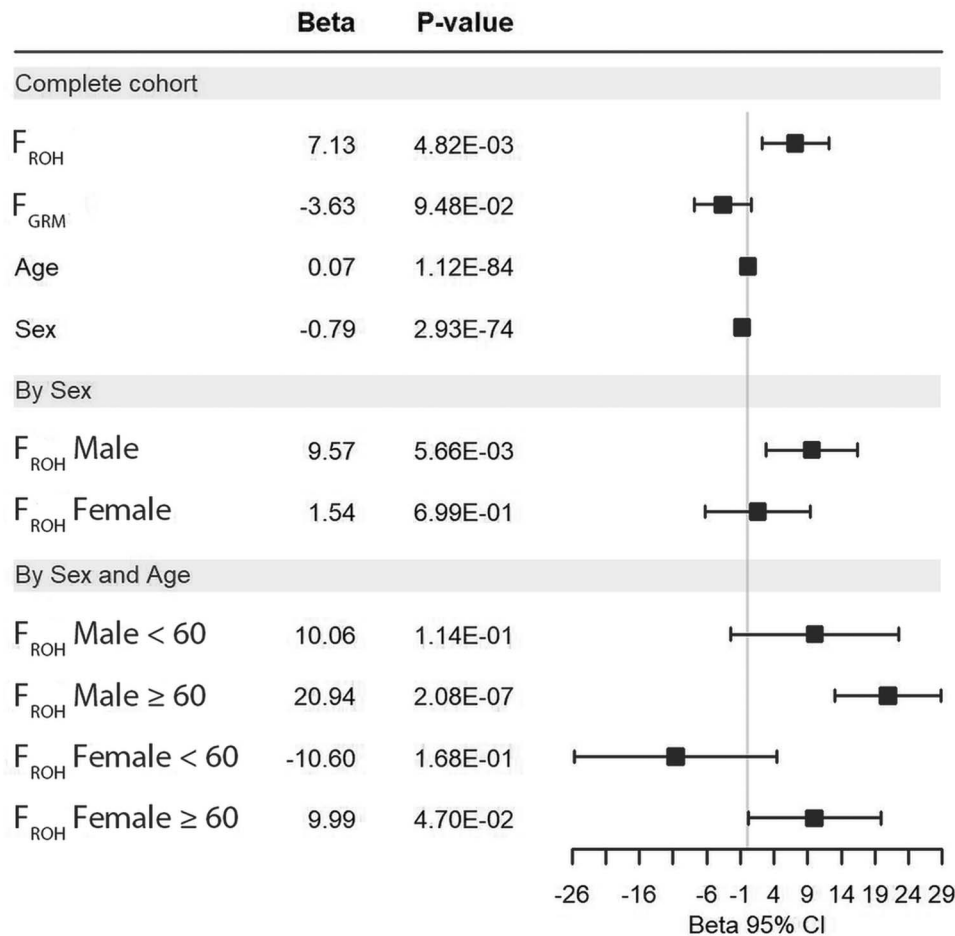


Figure 6. Effect of the ID on COVID-19 hospitalization in the SCOURGE cohort. Forest plots are shown for global analyses as well as for sex and age-disaggregated analyses.

for hospitalization and severity in males ≥ 60 years old, but it was marginally significant in females (Fig. 6 and Supplementary Material, Table S9). Age and sex-specific effects in hospitalization and severity were robust across different experimental designs using different control groups (Supplementary Material, Fig. S7).

Finally, we then aimed to replicate the ID results with hospitalization, assessing sex and age-specific effects, in a 4418 case-enriched European cohort made of 16 studies from nine countries. Median F_{ROH} in this other European cohort was slightly higher than that of SCOURGE, 0.05 (0.009–0.0577). A positive and significant ID in COVID-19 hospitalization was detected in this other European cohort when the entire cohort was considered (F_{ROH} Beta = 18.22, $P = 3.33 \times 10^{-3}$). F_{GRM} was not significant (F_{GRM} Beta = -7.34, $P = 0.240$). ID was also detected in hospitalized COVID-19 males but not in females (Male F_{ROH} Beta = 16.22, $P = 3.31 \times 10^{-3}$; Female F_{ROH} Beta = 15.65, $P = 0.269$). F_{GRM} was not significant in males or in female analyses. When disaggregating by age, it was possible to detect significant ID in hospitalization only in males ≥ 60 years old (F_{ROH} Beta = 36.16, $P = 3.34 \times 10^{-3}$) (Supplementary Material, Table S10).

No evidence was found of major loci that may be exerting large effects. Rather, polygenicity seems to underlie

the ID association. Different islands of ROH (ROHi) and regions of heterozygosity (RHZ) were found to be unique for hospitalized COVID-19 individuals (males and females) and non-hospitalized males, respectively (Supplementary Note, Supplementary Material, Table S11). Enrichment analysis of pathways based on the protein coding genes present in ROH islands were also different between sexes (Supplementary Note, Supplementary Material, Table S12), revealing links with coagulation and complement pathways in males.

Discussion

Here we report the replication of six COVID-19 loci across analyses and provide evidence supporting three additional loci, one of them specifically detected among females. Besides, our analyses provide new insights into disease severity disparities by sex and age and support the necessity of similarly stratified studies to increase the possibility of detecting additional risk variants. Our GWAS constitutes the largest study on COVID-19 genetic risk factors conducted in Spain, with an intrinsic design benefit that SCOURGE includes detailed clinical and genetic information gathered homogeneously across the country. Besides, the study

included patients from the whole spectrum of COVID-19 severity covering from asymptomatic to life-threatening disease. To date, most research on COVID-19 disease has focused on respiratory failure. However, the inclusion of a severity scale provided a unique opportunity to assess whether previously reported loci combined into a GRS model were associated with differential risk by strata. We warn, however, that the GRS model findings should be interpreted with caution as sex and age-differential results in some of the severity strata needs appropriate replication. Association was tested for four main variables: infection, hospitalization, severe illness and critical illness, and using different definitions of controls to align with the COVID-19 HGI. Irrespective of the tested outcomes or the definition of controls, the results were very similar, supporting the use of population controls to increase power in these studies and the utility of using hospitalization as a proxy of severity. However, our results from the GRS analysis reported a need to maintain separated categories for medium-severe and critical illness.

We observed larger heritability differences by age groups among males than among females for COVID-19 hospitalization, which have diverse support from the literature. On the one hand, there is robust evidence supporting that the presence of X-linked deleterious variants in the *TLR7* gene are causal for life-threatening COVID-19 only affecting males (19–21). Of note, most of these severe COVID-19 male patients were younger than 60 years (21). On the other hand, autoantibodies impairing type-I interferon signaling, which are supported to be strong determinants of critical COVID-19 pneumonia, are preferentially found among males older than 65 years (11,18). Taken together, this reconciles with the idea that non-genetic factors involved in severe COVID-19 are expected among older males.

We clearly replicated previously reported associations at 3p21.31 (near *SLC6A20* and *LZTFL1-FYCO1*) (7,9,22,23) and 21q22.11 (in *IFNAR2*) (7,9), and other findings in *ABO*, *OAS1*, *TYK2* and *ARHGAP27*. We also found a differential effect between males and females for SNPs in 3p21.31 and 21q22.11. Although in the meta-analysis with other European studies the leading variants of 3p21.31 reached genome-wide significance in females, there was still a difference in effect size that, considering its magnitude, should not be disregarded. It is important to remark that these association signals found in males were not associated with the presence of comorbidities (see [Supplementary Material, Fig. S4](#)). In fact, genetic effects were only found for younger males (<60 years old), consistent with other studies (24) and strongly supporting those comorbidities outweigh genetic effects in disease outcomes in the older patients.

Some novel genome-wide significant signals were found in our study, one in chromosome 19q13.12 (intergenic to *UPK1A* and *ZBTB32*, and also linked to the transcriptional regulation of *ARHGAP33*), and another in chromosome 9p13.3 (intergenic to *AQP7* and *AQP3*).

Interestingly, we also found two sex-specific signals: *ELF5* in males and *TLE1* in females. *ELF5* has been recently reported as a new locus associated with critical illness in Europeans (25). Variants of this locus reached genome-wide significance in our male meta-analysis of European cohorts ($P = 4.1 \times 10^{-8}$). As regards of *TLE1*, this locus should be taken as speculative as the signal did not reach the standard genome-wide significance in the study. However, given that the meta-analysis involved a low number of studies (and the top marker was not imputed in one of them), this result should be taken with caution as further sex-specific studies will be needed to validate this finding.

TLE1 encodes for the transducin-like enhancer of split 1, a co-repressor of other transcription factors and signaling pathways. Besides repressing the transcriptional activity of *FOXA2* and of the Wnt signaling, *TLE1* has been shown to negatively regulate *NF-κB*, which is fundamental in controlling inflammation and the immune response. The deficiency of *TLE1* activity in mice results in enhancement of the *NF-κB*-mediated inflammatory response in diverse tissues including the lung (26). Interestingly, *TLE1* is one of the 332 high-confidence SARS-CoV-2 protein-human protein interactions identified so far (27). Taken together, SARS-CoV-2 would be directly targeting the innate immunity and inflammation signaling pathways by interfering with the *NF-κB* activity. Thus, it is not surprising that *TLE1* is a top-ranking regulator of inflammation that allows to transcriptionally distinguish mild from severe COVID-19 (28).

In the 19q13.12 locus, the most biologically plausible genes are *ARHGAP33* (also showing the best functional support based on the fine-mapping variants) and *ZBTB32*. *ARHGAP33* is transcriptionally regulated by *IRF1*—a prominent antiviral effector and IFN-stimulated gene (29). It also harbors *NF-κB* binding site that modifies its expression in human lymphoblastoid cell lines by the presence of genetic variants in the binding site linked to many inflammatory and immune-related diseases including sepsis, and bacterial and viral infection (30). Its expression is also altered in human induced pluripotent stem cells-derived pancreatic cultures in response to SARS-CoV-2 infection (31). *ARHGAP33* was identified in an unbiased genome-wide CRISPR-based knockout screen in human Huh7.5.1 hepatoma cells infected by coronaviruses including SARS-CoV-2 and further interactome studies (32). With respect to the transcription factor *ZBTB32*, it has been shown to impair antiviral immune responses by affecting cytokine production and the proliferation of natural killer and T cells, and the generation of memory cells (33). In single cell studies, transcripts of *ZBTB32* were enriched in T follicular helper cells and were also expressed at significantly higher levels in hospitalized COVID-19 patients (34).

AQP3 is expressed most strongly in the kidney collecting duct, the gastrointestinal tract, large airways (in basal epithelial cells and the nasopharynx), skin and the urinary bladder; whereas *AQP7* is expressed

primarily in the testis, fat cells and, to a lesser extent in a subsegment of the kidney proximal tubule (35). In addition, AQP3 is upregulated in the lung tissues during viral or bacterial-induced diffuse alveolar damage (36). Based on this, in the fact that SARS-CoV-2 interacts with host proteins with the highest expression in lung tissues (27), and the functional evidence linking the fine-mapped variants with eQTLs in lung tissues, our data support AQP3 as the most likely 9p13.3 gene driving the association with COVID-19 hospitalization. Many patients develop acute respiratory distress syndrome (ARDS) during severe COVID-19 (37), and one of the hallmarks of ARDS is the increase of fluid volume (edema) in the airspaces of the lung because of an increase in the alveolo-capillary membrane permeability. Some of the aquaporins, including AQP3, essentially function as water transport pores between the airways and the pulmonary capillaries (38), are key in lung fluid clearance and the formation of this lung edema as a consequence of the lung injury (35). In fact, the use of aquaporin modulators in lung inflammation and edema has been proposed for potential use for the treatment of COVID-19 respiratory comorbidity (39).

We have also shown for the first time that COVID-19 severity risk suffers from ID, where individuals with higher levels of homozygosity associate with higher risk of being hospitalized and of developing severe COVID-19. Our results also suggested that autozygous rare recessive variants found in ROH across the genome, rather than homozygous common variants in strong LD, are underlying the ID. Furthermore, the ID is stronger in males than in females suffering from COVID-19 hospitalizations, especially in males ≥ 60 years old. Although these results may be found counterintuitive with the rest of findings, they are supported by the mutation accumulation senescence theory. Under this theory, alleles with detrimental effects that act in late life are expected to accumulate and cause senescence, thus increasing the ID (40). We detected further sex-specific effects of homozygosity through ROHi. In hospitalized males, coagulation and complement pathways, which have been previously associated with severe COVID-19 (41), were enriched among the protein coding genes located in ROHi, highlighting the role of homozygosity whereas the Lectin pathway of complement activation is reported to be involved in the response to SARS-CoV-2 infection (42–44). In hospitalized females, PI3K-Akt signaling genes were found to be enriched in ROH islands, whose networks are affected by a great variety of viruses (45).

Given that the effect of the genetic variants in SARS-CoV-2 severity is clearer among males and previous evidence on this regard, we elucidate on the role of androgens in COVID-19 severity. Androgenic hormones have been suggested to be responsible of the excess male mortality observed in COVID-19 patients (46), and several lines of evidence suggest that the androgen receptor (AR) pathway is involved in the severity of SARS-CoV-2

infection: (i) A higher mortality rate among men has been established (47); (ii) A substantial proportion of individuals, both males and females, hospitalized for severe COVID-19 have androgenetic alopecia [AGA; (47)] and (iii) Most of the genes on COVID-19 severity in this study have been identified in male-only analyses, and these genes have been shown to interact with the AR. The following lines of evidence suggest the AR pathway is a mechanism responsible for some identified genes-COVID-19 severity relationship: (i) FYCO1 is regulated by the AR (48), and binding sites between the sex hormone receptor AR and FYCO1 have been demonstrated (48,49); (ii) There is a cross-talk between the IFN pathways and the androgen signaling pathways (50), and androgens are regulated by IFNs in human prostate cells (51); (iii) TMPRSS2, another gene associated with COVID-19 severity in other studies, is induced by androgens through a distal AR binding enhancer (52); (iv) AR induces the expression of chemokine receptors such as CCR1; (v) Variants of LZTFL1 gene are likely pathogenic for male reproductive system diseases (53) and (vi) Genetic polymorphisms in the AR (long polyQ alleles ≥ 23) and higher testosterone levels in subjects with AR long-polyQ appear to predispose some men to develop more severe disease (54). Thus, it is not unexpected to find that antiandrogen treatments are under the focus as treatment options and prophylaxis of severe COVID-19 (47) and that randomized controlled clinical trials with bicalutamide (NCT04374279), degarelix (NCT04397718) and spironolactone (NCT04345887) are currently underway.

Materials and Methods

Recruitment of cases and phenotype definitions for the discovery phase

In Spain, 11 939 COVID-19 positive cases were recruited as part of SCOURGE study from 34 centers in 25 cities between March and December 2020. The complete list of hospitals or research centers and the number of samples that each contributed to the study is shown in [Supplementary Material, Table S1](#). Study samples and data were collected by the participating centers, through their respective biobanks after informed consent, with the approval of the respective Ethic and Scientific Committees. The whole project was approved by the Galician Ethical Committee Ref 2020/197. All samples and data were processed following normalized procedures. Study data were collected and managed using REDCap electronic data capture tools hosted at Centro de Investigación Biomédica en Red [CIBER; (55,56); [Supplementary Material, Supplemental Note](#)]. Individuals were diagnosed as COVID-19 positive through a PCR-based test (81.7% of cases) or according to local clinical (3.4%) and laboratory procedures (antibody test: 14.2%; other microbiological tests: 0.7%). All cases were classified in a five-level severity scale ([Table 1](#)).

Two Spanish sample collections with unknown COVID-19 status were included as general population controls

in some analyses: 3437 samples from the Spanish DNA biobank (<https://www.bancoadn.org>) and 2506 samples from the GR@CE consortium (17). General population controls were collected from branches of the National Blood Service from adult unrelated individuals self-reporting Spanish origin and absence of personal and familial history of diseases including infectious, cancerous, blood and circulatory, endocrine, mental or behavioral, nervous, vision, hearing, respiratory, immunological, bone, congenital, skin and digestive.

Second phase: the CNIO study

A total of 1598 COVID-19 cases from six different Spanish Biobanks (Biobanco CNIO, Biobanco Vasco, Biobanco Hospital Ramón y Cajal, Biobanco Hospital Puerta de Hierro, Biobanco Hospital San Carlos, and Banco Nacional de ADN) were obtained according to the ethical committee approval CEI PI 34_2020-v2. In addition, 1068 individuals from Spanish DNA biobank with unknown COVID-19 status were included as healthy controls in the analysis whenever necessary. Classification as healthy was based on self-reported absence of cardiovascular, renal, pulmonary, hepatic, hematological illnesses or any other chronic conditions, which require continuous treatment, hepatitis B, C infections or acquired immunodeficiency syndrome (AIDS). No clinical characterization was performed on any subject, no information from medical record was incorporated and no medical testing was performed on these individuals. We will refer to these cases and controls as the Centro Nacional de Investigaciones Oncológicas (CNIO) study.

Genotyping

The discovery phase samples were genotyped with the Axiom Spain Biobank Array (Thermo Fisher Scientific) following the manufacturer's instructions in the Santiago de Compostela Node of the National Genotyping Center (CeGen-ISCI; <http://www.usc.es/cegen>). This array contains 757 836 markers, including rare variants selected in the Spanish population. Genomic DNA was obtained from peripheral blood and isolated using the Chemagic DNA Blood100 kit (PerkinElmer Chemagen Technologies GmbH), following the manufacturer's recommendations.

For the second phase study samples, a total of 250 ng of DNA was processed according to the Infinium HTS assay Protocol (Part # 15045738 Rev. A, Illumina), including amplification, fragmentation and hybridization using the Global Screening Array Multi-disease v3.0. This array contains a total of 730 059 markers and was scanned on an iScan platform (Illumina, Inc.). Clustering and genotype calling were performed using Genome Studio v2.0.4 (Illumina, Inc.).

Quality control

A QC procedure was carried out for the SCOURGE study samples and control datasets. First, a list of probe sets

was removed based on poor cluster separation or excessive MAF difference from The 1000 Genomes Project data (1KGP) (57). Then, the following QC steps were applied using PLINK 1.9 (58) and a custom R script. We excluded variants with $MAF < 1\%$, call rate $< 98\%$, a difference in missing rate between cases and controls > 0.02 , or deviating from Hardy–Weinberg equilibrium (HWE) expectations [$P < 1 \times 10^{-6}$ in controls, $P < 1 \times 10^{-10}$ in cases, with a mid-P adjustment (59)]. Samples with a call rate $< 98\%$ and those in which heterozygosity rate deviated > 5 SD from the mean heterozygosity of the study were also removed.

To assess kinship and assign ancestries, autosomal SNPs ($MAF > 5\%$) were pruned with PLINK using a window of 1000 markers, a step size of 80 and a r^2 of 0.1. In addition, high-linkage disequilibrium (LD) regions described in Price *et al.* (60) were also excluded. A subset of 131 937 independent SNPs was used to evaluate kinship (IBD estimation) in PLINK. Given the possible confusion between relatedness and ancestry, we removed only one individual from each pair of individuals with $PI_HAT > 0.25$ (second-degree relatives) that showed a Z0, Z1 and Z2 coherent pattern (according to theoretical expected values for each relatedness level). The unrelated SCOURGE individuals were merged with samples from 1KGP and the common SNPs were LD-pruned as previously indicated. Ancestry was then inferred with Admixture (61) using the defined 1KGP superpopulations. Those individuals with an estimated probability $> 80\%$ of pertaining to European ancestry were defined as European ($N = 15\,571$).

Genomic PCs were also computed using a LD-pruned ($r^2 < 0.1$ with a window size of 1000 markers) subset of genotyped SNPs passing quality check for controlling the population structure in the GWAS.

The CNIO study data was filtered following the same QC procedures, where 220 individuals were identified as non-European and, therefore, were excluded from further analysis.

Variant imputation

Imputation was conducted based on the TOPMed version r2 reference panel [GRCh38; (62)] in the TOPMed Imputation Server. After post-imputation filtering ($Rsq > 0.3$, HWE $P > 1 \times 10^{-6}$, $MAF > 1\%$), 15 045 individuals (9371 COVID-19 positive cases and 5674 population controls) and 8 933 154 genetic markers remained in the SCOURGE European study (discovery). The final dataset of the CNIO study (replication) included 2446 individuals (1378 COVID-19 positive cases and 1068 population controls) and 8 895 721 markers. For directly genotyped variants, the original genotype was maintained in place of the imputed data.

Statistical analysis

Association testing was computed by fitting logistic mixed regression models adjusting for age, sex and the first 10 ancestry-specific PCs. SNPRelate (63) was

used for prior LD-pruning and data management. Association analyses were performed in SAIGE (64), which implements the SAIGE (65) two-step mixed model methodology and the SPA test while using more efficient objects for genotype storage. A null model was fitted in the first step using the LD-pruned genotyped variants ($MAF > 0.5\%$, missing rate $< 98\%$) to estimate variance components and the genetic relationship matrix. Then, in a second step, association analyses were performed for both genotyped and imputed SNPs. Significance was established at $P < 5 \times 10^{-8}$ after meta-analysis of the discovery and the second study phases.

To align the results with those from the COVID-19 HGI, three outcomes were evaluated in relation to severity: hospitalization, severe COVID-19 (severity ≥ 3) and very severe COVID-19 (severity = 4, critical illness). For each comparison, three control definitions (A1, A2 and C) were used (Supplementary Material, Table S2).

In addition, the risk to COVID-19 infection was also analysed by comparing all COVID-19 positive cases with control samples from the general population.

All analyses were conducted for each complete dataset and stratified by sex and age (< 60 years, ≥ 60 years). The SNP*sex and SNP*age-interaction terms were tested for each SNP in the subset of clumped signals, adjusting the models for the same covariates.

Then, the main results of both Spanish cohorts (SCOURGE and CNIO) for the overall and sex-stratified analyses were meta-analysed assuming a fixed-effects model using METAL (66).

Because of the similarity of both the SCOURGE and CNIO studies in the clinical variables recorded and, more importantly, in the definition of the severity scale, the leading variants from the significant and validated loci in the hospitalization analysis were also analysed under a multinomial model (Supplementary Material, Supplemental Note).

Meta-analysis in independent European studies

In order to validate the findings in independent study samples of European ancestry, a meta-analysis of hospitalization risk was performed for the overall and sex-stratified summary statistics of both Spanish cohorts (SCOURGE and CNIO) and other four sex-stratified Europeans studies from the COVID-19 HGI consortium (Bel-COVID, GenCOVID, Hostage-Spain and Hostage-Italy).

Bayesian fine-mapping of GWAS findings

Credible sets were calculated for the GWAS loci to identify a subset of variants most likely containing the causal variant at 95% confidence level, assuming that there is a single causal variant and that it has been tested. We used *corrcoverage* for R (67) to calculate the posterior probabilities of the variant being causal for all variants with $r^2 > 0.1$ with the leading SNP and within 1 Mb. Variants were added to the credible set until the sum of the posterior probabilities was ≥ 0.95 . VEP (<https://www.ensembl.org/info/docs/tools/vep/index.html>) and

the V2G aggregate scoring from Open Targets Genetics (<https://genetics.opentargets.org>) were used to annotate the most prominent biological effects of the variants in the credible sets.

Genetic risk score

A GRS was created for the SCOURGE cohort individuals and population controls using the list of SNPs associated with hospitalization, severity or risk in the meta-analysis performed by the COVID-19 HGI [see Supplementary Material, Table S2 in (9)] to appraise its prediction power of the severity scale in SCOURGE. Details of this analysis can be found in Supplementary Note.

SNP-heritability of COVID-19 severity

We relied on GCTA-GREML 1.93.2beta (68) to assess the heritability of severe COVID-19 symptoms among SCOURGE patients, excluding those with cryptic relatedness or with missing genotypes above 0.5% and assuming a prevalence of COVID-19 hospitalization of 0.5%. This analysis considered all patients (modelling for age, sex, sex*age and the 10 first PCs), and males and females separately (modelling for age and the 10 first PCs). We also partitioned the variance to assess the heritability changes among the patients < 60 or ≥ 60 years old. We focused on the 547 206 autosomal variants with $MAF > 1\%$ and missingness $< 0.5\%$. Assuming 0.5% of prevalence of severe COVID-19, and at least 1500 cases and 1500 controls per stratum, we estimate $> 97.9\%$ power to detect a heritability > 0.2 .

ROH calling

The ROH segments longer than 300 Kb were called in SCOURGE using PLINK 1.9 in the European QC-ed genotyped dataset (before imputation) with the following parameters: *homozyg-snp* 30, *homozyg-kb* 300, *homozyg-density* 30, *homozyg-window-sn* 30, *homozyg-gap* 1000, *homozyg-window-het* 1, *homozyg-window-missing* 5 and *homozyg-window-threshold* 0.05. No LD pruning was performed.

Calculating genomic inbreeding coefficients

Different genomic inbreeding coefficients were calculated (69):

F_{ROH} measures the actual proportion of the autosomal genome that is autozygous above a specific threshold of minimum ROH length.

$$F_{ROH} = \frac{\sum_{i=1}^n ROH > 1.5 \text{ Mb}}{3 \text{ Gb}}$$

F_{GRM} is an alternative genomic inbreeding coefficient that was obtained using PLINK's parameter *-ibc* (Fhat3). This coefficient is described by Yang et al. (68) where N is the number of SNPs, p_i is the reference allele frequency of the i th SNP, and x_i is the number of copies of the reference allele. The reference allele frequencies were site-specific

and included only variants with MAF > 0.05.

$$F_{\text{GRM}} = \frac{1}{N} \sum_i^n \frac{(x_i^2 - (1 + 2p_i)x_i + 2p_i^2)}{2p_i(1 - p_i)}$$

Testing and replicating the ID

Inbreeding depression is defined as the change in the mean phenotypic value in a population because of inbreeding (12,13). The ID was modelled in SCOURGE by a multiple logistic regression. The covariables used in this study were sex, age and the first 10 PCs.

The results were replicated in a cohort gathered by Nakanishi et al. (24). This consists of clinical and genomic data from 4418 individuals of European ancestry (3946 hospitalized COVID-19 cases and 422 controls): 2597 males (1072 males < 60 years old, 1525 males ≥ 60 years old) and 1821 females (808 females < 60 years old, 1013 females ≥ 60 years old). The cohort was built by harmonizing individual-level data from 16 different studies (24). The F_{ROH} and F_{GRM} coefficients were obtained following the procedure explained previously. The model described previously with the same covariables (age, sex and the first then PCs) was applied in this cohort.

Genome-specific effects on COVID-19 severity and hospitalization were tested through ID in genomic windows, ROH islands (ROHi) and regions of heterozygosity (RHZ) (Supplementary Material, Supplemental Note).

Supplementary Material

Supplementary Material is available at HMGJ online.

Acknowledgements

R.L.-R. is granted by Cátedra de Medicina Genómica IIS-Fundación Jiménez Díaz-UAM, M.B. by Nextgeneration EU funds. M.C., P.M., M.A.J.S., A.F.R. are granted by the Miguel Servet Programme (CP17/00006, CP16/00116, CPII20CIII/0001, CPII20CIII/0001 respectively) and B.A. by the Juan Rodés Programme (JR17/00020), all of them from Instituto de Salud Carlos III, and cofunded by European Union (ERDF) 'A way of making Europe'.

The contribution of the Centro Nacional de Genotipado (CEGEN), and Centro de Supercomputación de Galicia (CESGA) for funding this project by providing supercomputing infrastructures, is also acknowledged. Authors are also particularly grateful for the supply of material and the collaboration of patients, health professionals from participating centers and biobanks. Namely Biobanc-Mur, and biobancs of the Complejo Hospitalario Universitario de A Coruña, Complejo Hospitalario Universitario de Santiago, Hospital Clínico San Carlos, Hospital La Fe, Hospital Universitario Puerta de Hierro Majadahonda—Instituto de Investigación Sanitaria Puerta de Hierro—Segovia de Arana, Hospital Ramón y Cajal, IDIBGI, IdISBa, IIS Biocruces Bizkaia, IIS Galicia Sur. Also biobanks of the

Sistema de Salud de Aragón, Sistema Sanitario Público de Andalucía, and Banco Nacional de ADN.

SCOURGE Cohort Group members and affiliations, HOSTAGE Cohort Group and GR@ACE Cohort Group (Supplementary Material).

Conflict of Interest statement: The authors declare no competing interests.

Funding

Instituto de Salud Carlos III (COV20_00622 to A.C., COV20/00792 to M.B., COV20_00181 to C.A., COV20_1144 to M.A.J.S., PI20/00876 to C.F.); European Union (ERDF) 'A way of making Europe'. Fundación Amancio Ortega, Banco de Santander (to A.C.), Estrella de Levante S.A. and Colabora Mujer Association (to E.G.-N.) and Obra Social La Caixa (to R.B.); Agencia Estatal de Investigación (RTC-2017-6471-1 to C.F.), Cabildo Insular de Tenerife (CGIEU0000219140 'Apuestas científicas del ITER para colaborar en la lucha contra la COVID-19' to C.F.) and Fundación Canaria Instituto de Investigación Sanitaria de Canarias (PIFIISC20/57 to C.F.).

References

1. Tang, D., Komish, P. and Kang, R. (2020) The hallmarks of COVID-19 disease. *PLoS Pathog.*, **16**, e1008536. <https://doi.org/10.1371/journal.ppat.1008536>.
2. Goyal, P., Choi, J., Pinheiro, L., Schenck, E., Chen, R., Jabri, A., Satlin, M., Campion, R., Nahid, M., Ringel, J. et al. (2020) Clinical characteristics of Covid-19 in new York City. *N. Engl. J. Med.*, **382**, 2372–2374.
3. Richardson, S., Hirsch, J., Narasimhan, M., Crawford, J., McGinn, T., Davidson, K. and the Northwell COVID-19 Research Consortium (2020) Presenting characteristics, comorbidities, and outcomes among 5700 patients hospitalized with COVID-19 in the New York City area. *JAMA*, **323**, 2052–2059.
4. Vahidy, F., Pan, A., Ahnstedt, H., Munshi, Y., Choi, H., Tiruneh, Y., Nasir, K., Kash, B., Andrieni, J. and McCullough, L. (2021) Sex differences in susceptibility, severity, and outcomes of coronavirus disease 2019: cross-sectional analysis from a diverse US metropolitan area. *PLoS One*, **16**, e0245556. <https://doi.org/10.1371/journal.pone.0245556>.
5. The COVID-19 Host Genetics Initiative (2020) The COVID-19 host genetics initiative, a global initiative to elucidate the role of host genetic factors in susceptibility and severity of the SARS-CoV-2 virus pandemic. *Eur. J. Hum. Genet.*, **28**, 715–718.
6. Casanova, C., Su, H. and COVID Human Genetic Effort (2020) A global effort to define the human genetics of protective immunity to SARS-CoV-2 infection. *Cell*, **181**, 1194–1199.
7. Pairo-Castineira, E., Clohisey, S., Klaric, L., Bretherick, A., Rawlik, K., Pasko, D., Walker, S., Parkinson, N., Fourman, M., Russell, C. et al. (2021) Genetic mechanisms of critical illness in COVID-19. *Nature*, **591**, 92–98.
8. Zhang, Q., Bastard, B., Liu, Z., Le Pen, J., Moncada-Velez, M., Chen, J., Ogishi, M., Sabli, I., Hodeib, S., Korol, C. et al. (2020) Inborn errors in type I IFN immunity in patients. *Science*, **370**, eabd4570. <https://doi.org/10.1126/science.abd4570>.
9. COVID-19 Host Genetics Initiative (2021) Mapping the human genetic architecture of COVID-19. *Nature*, **600**, 472–477.

10. Brady, E., Nielsen, M., Andersen, J. and Oertelt-Prigione, S. (2021) Lack of consideration of sex and gender in COVID-19 clinical studies. *Nat. Commun.*, **12**, 4015. <https://doi.org/10.1038/s41467-021-24265-8>.
11. Bastard, P., Rosen, L., Zhang, Q., Michailidis, E., Hoffmann, H., Dorgham, Z., Philippot, Q., Rosain, J., Béziat, V., Manry, J. et al. (2020) Autoantibodies against type I IFNs in patients with life-threatening COVID-19. *Science*, **370**, eabd4570. <https://doi.org/10.1126/science.abd4585>.
12. Charlesworth, D. and Willis, H. (2009) The genetics of inbreeding depression. *Nat. Rev. Genet.*, **10**, 783–796.
13. Ceballos, F., Joshi, P., Clark, D., Ramsay, M. and Wilson, J. (2018) Runs of homozygosity: windows into population history and trait architecture. *Nat. Rev. Genet.*, **19**, 220–234.
14. Ceballos, F., Hazelhurst, S., Clark, D., Agongo, G., Asiki, G., Boua, P., Gómez-Olivé, X., Mashinya, F., Norris, S., Wilson, J. et al. (2020) Autozygosity influences cardiometabolic disease-associated traits in the AWI-gen sub-Saharan African study. *Nat. Commun.*, **11**, 5754. <https://doi.org/10.1038/s41467-020-19595-y>.
15. Clark, D., Okada, Y., Moore, K., Mason, D., Pirastu, N., Gandin, I., Mattsson, H., Barnes, C., Lin, K., Zhao, J. et al. (2019) Associations of autozygosity with a broad range of human phenotypes. *Nat. Commun.*, **10**, 4957. <https://doi.org/10.1038/s41467-019-12283-6>.
16. Moreno-Grau, S., Fernández, M., de Rojas, I., García-González, P., Hernández, I., Fariás, F., Budde, J., Quintela, I., Madrid, L., González-Pérez, A. et al. (2021) Long runs of homozygosity are associated with Alzheimer's disease. *Transl. Psychiatry*, **11**, 142. <https://doi.org/10.1038/s41398-020-01145-1>.
17. Moreno-Grau, S., de Rojas, I., Hernández, I., Quintela, I., Montreal, L., Alegret, M., Hernández-Olasagarre, B., Madrid, L., González-Pérez, A., Maroñas, O. et al. (2019) Genome-wide association analysis of dementia and its clinical endophenotypes reveal novel loci associated with Alzheimer's disease and three causality networks: the GR@ACE project. *Alzheimers Dement.*, **15**, 1333–1347.
18. Bastard, P., Gervais, A., Le Voyer, T., Rosain, J., Philippot, Q., Manry, J., Michailidis, E., Hoffmann, H., Eto, S., García-Prat, M. et al. (2021) Autoantibodies neutralizing type I IFNs are present in ~4% of uninfected individuals over 70 years old and account for ~20% of COVID-19 deaths. *Sci. Immunol.*, **6**, EABL4340. <https://doi.org/10.1126/sciimmunol.abl4340>.
19. van der Made, C., Simons, A., Schuurs-Hoeijmakers, J., van den Heuvel, G., Mantere, T., Kersten, S., van Deuren, R., Steehouwer, M., van Reijmersdal, S., Jaeger, M. et al. (2020) Presence of genetic variants among young men with severe COVID-19. *JAMA*, **324**, 663–673.
20. Fallerini, C., Daga, S., Mantovani, S., Benetti, E., Picchiotti, N., Francisci, D., Paciosi, F., Schiaroli, E., Baldassarri, M., Fava, F. et al. (2021) Association of Toll-like receptor 7 variants with life-threatening COVID-19 disease in males: findings from a nested case-control study. *Elife*, **10**, e67569. <https://doi.org/10.7554/eLife.67569>.
21. Asano, T., Boisson, B., Onodi, F., Matuozzo, D., Moncada-Velez, M., Maglorius Renkilaraj, M., Zhang, P., Meertens, L., Bolze, A., Materna, M. et al. (2021) X-linked recessive TLR7 deficiency in ~1% of men under 60 years old with life-threatening COVID-19. *Sci. Immunol.*, **6**, eabl4348. <https://doi.org/10.1126/sciimmunol.abl4348>.
22. Severe Covid-19 GWAS Group, Ellinghaus, D., Degenhardt, F., Bujanda, L., Buti, M., Albillos, A., Invernizzi, P., Fernández, J., Prati, D., Baselli, G. et al. (2020) Genomewide association study of severe Covid-19 with respiratory failure. *N. Engl. J. Med.*, **383**, 1522–1534.
23. Shelton, J., Shastri, A., Ye, C., Weldon, C., Filshtein-Sonmez, T., Coker, D., Symons, A., Esparza-Gordillo, J., 23andMe COVID-19 Team, Aslibekyan, S. et al. (2021) Trans-ancestry analysis reveals genetic and nongenetic associations with COVID-19 susceptibility and severity. *Nat. Genet.*, **53**, 801–808.
24. Nakanishi, T., Pigazzini, S., Degenhardt, F., Cordioli, M., Butler-Laporte, G., Maya-Miles, D., Bujanda, L., Bouysran, Y., Niemi, M., Palom, A. et al. (2021) Age-dependent impact of the major common genetic risk factor for COVID-19 on severity and mortality. *J. Clin. Invest.*, **131**, e152386. <https://doi.org/10.1172/JCI152386>.
25. Kousathanas, A., Pairo-Castineira, E., Rawlik, K., Stuckey, A., Odhams, C., Walker, S., Russell, C., Malinauskas, T., Millar, J., Elliott, K. et al. (2022) Whole genome sequencing reveals host factors underlying critical Covid-19. *Nature*. <https://doi.org/10.1038/s41586-022-04576-6>.
26. Ramasamy, S., Saez, B., Mukhopadhyay, S., Ding, D., Ahmed, A., Chen, X., Pucci, F., Yamin, R., Wang, J., Pittet, M. et al. (2016) Tle1 tumor suppressor negatively regulates inflammation in vivo and modulates NF- κ B inflammatory pathway. *PNAS*, **113**, 1871–1876.
27. Gordon, D., Jang, G., Bouhaddou, M., Xu, J., Obernier, K., White, K., O'Meara, M., Rezeli, V., Guo, J., Swaney, D. et al. (2020) A SARS-CoV-2 protein interaction map reveals targets for drug repurposing. *Nature*, **583**, 459–468.
28. de Jong, T., Guryev, V. and Moshkin, Y. (2021) Estimates of gene ensemble noise highlight critical pathways and predict disease severity in H1N1, COVID-19 and mortality in sepsis patients. *Sci. Rep.*, **11**, 10793. <https://doi.org/10.1038/s41598-021-90192-9>.
29. Schoggins, J. and Rice, C. (2011) Interferon-stimulated genes and their antiviral effector functions. *Curr. Opin. Virol.*, **1**, 519–525.
30. Karczewski, K., Dudley, J., Kukurba, K., Chen, R., Butte, A., Montgomery, S. and Snyder, M. (2013) Systematic functional regulatory assessment of disease-associated variants. *PNAS*, **110**, 9607–9612.
31. Shaharuddin, S., Wang, V., Santos, R., Gross, A., Wang, Y., Jawanda, H., Zhang, Y., Hasan, W., Garcia, G., Jr., Arumugaswami, V. et al. (2021) Deleterious effects of SARS-CoV-2 infection on Human pancreatic cells. *Front. Cell. Infect. Microbiol.*, **11**, 678482. <https://doi.org/10.3389/fcimb.2021.678482>.
32. Wang, R., Simoneau, C., Kulsuptrakul, J., Bouhaddou, M., Travisanò, K., Hayashi, J., Carlson-Stevermer, J., Zengel, J., Richards, C., Fozouni, P. et al. (2021) Genetic screens identify host factors for SARS-CoV-2 and common cold coronaviruses. *Cell*, **184**, 106–119.
33. Shin, H., Kapoor, V., Kim, G., Li, P., Kim, H., Suresh, M., Kaech, S., Wherry, E., Selin, L., Leonard, W., Welsh, R.M. and Berg, L.J. (2017) Transient expression of ZBTB32 in anti-viral CD8⁺ T cells limits the magnitude of the effector response and the generation of memory. *PLoS Pathog.*, **13**, e1006544. <https://doi.org/10.1371/journal.ppat.1006544>.
34. Beaulieu, A., Zawislak, C., Nakayama, T. and Sun, J. (2014) The transcription factor Zbtb32 controls the proliferative burst of virus-specific natural killer cells responding to infection. *Nat. Immunol.*, **15**, 546–553.
35. Song, Y., Fukuda, N., Bai, C., Ma, T., Matthay, M. and Verkman, A. (2000) Role of aquaporins in alveolar fluid clearance in neonatal and adult lung, and in oedema formation following acute lung injury: studies in transgenic aquaporin null mice. *J. Physiol.*, **525**, 771–779.
36. Pires-Neto, R., Del Carlo Bernardi, F., Alves de Araujo, P., Mauad, T. and Dolhnikoff, M. (2016) The expression of water and ion channels in diffuse alveolar damage is not dependent on DAD Etiology. *PLoS One*, **11**, e0166184. <https://doi.org/10.1371/journal.pone.0166184>.

37. Ferrando, C., Suarez-Sipmann, F., Mellado-Artigas, R., Hernández, M., Gea, A., Arruti, E., Aldecoa, C., Martínez-Pallí, G., Martínez-González, M., Slutsky, A. et al. (2020) Clinical features, ventilatory management, and outcome of ARDS caused by COVID-19 are similar to other causes of ARDS. *Intensive Care Med.*, **46**, 2200–2211.
38. Mariajoseph-Antony, L.F., Kannan, A., Panneerselvam, A., Loganathan, C., Anbarasu, K. and Prahalathan, C. (2020) Aquaporin water channels and lung physiology. *Am. J. Physiol. Lung Cell Mol.*, **278**, L867–L879.
39. Mariajoseph-Antony, L., Kannan, A., Panneerselvam, A., Loganathan, C., Anbarasu, K. and Prahalathan, C. (2020) Could aquaporin modulators be employed as prospective drugs for COVID-19 related pulmonary comorbidity? *Med. Hypotheses*, **143**, 110201. <https://doi.org/10.1016/j.mehy.2020.110201>.
40. Charlesworth, B. (2001) Patterns of age-specific means and genetic variances of mortality rates predicted by the mutation-accumulation theory of ageing. *J. Theor. Biol.*, **210**, 47–65.
41. Perico, L., Benigni, A., Casiraghi, F., Ng, L., Renia, L. and Remuzzi, G. (2021) Immunity, endothelial injury and complement-induced coagulopathy in COVID-19. *Nat. Rev. Nephrol.*, **17**, 46–64.
42. Java, A., Apicelli, A., Liszewski, M., Coler-Reilly, A., Atkinson, J., Kim, A. and Kulkarni, H. (2020) The complement system in COVID-19: friend and foe? *JCI Insight*, **5**, e140711. <https://doi.org/10.1172/jci.insight.140711>.
43. Lo, M., Kemper, C. and Woodruff, T. (2020) COVID-19: complement, coagulation, and collateral damage. *J. Immunol.*, **205**, 1488–1495.
44. Noris, M., Benigni, A. and Remuzzi, G. (2020) The case of complement activation in COVID-19 multiorgan impact. *Kidney Int.*, **98**, 314–322.
45. Dunn, E. and Connor, J. (2012) Chapter 9—HijAkt: the PI3K/Akt pathway in virus replication and pathogenesis. *Prog. Mol. Biol. Transl. Sci.*, **106**, 223–250.
46. Lamy, P., Rébillard, X., Vacherot, F. and de la Taille, A. (2021) Androgenic hormones and the excess male mortality observed in COVID-19 patients: new convergent data. *World J. Urol.*, **39**, 3121–3123.
47. Wambier, C., Goren, A., Vaño-Galván, S., Müller, P., Ossimetha, A., Nau, G., Herrera, S. and McCoy, J. (2020) Androgen sensitivity gateway to COVID-19 disease severity. *Drug Dev. Res.*, **81**, 771–776.
48. Shang, D., Wang, L., Klionsky, D., Cheng, H. and Zhou, R. (2021) Sex differences in autophagy-mediated diseases: toward precision medicine. *Autophagy*, **17**, 1065–1076.
49. Wyce, A., Bai, Y., Nagpal, S. and Thompson, C. (2010) Research resource: the androgen receptor modulates expression of genes with critical roles in muscle development and function. *Mol. Endocrinol.*, **24**, 1665–1674.
50. Bettoun, D., Scafonas, A., Rutledge, S., Hodor, P., Chen, O., Gambone, C., Vogel, R., McElwee-Witmer, S., Bai, C., Freedman, L. et al. (2005) Interaction between the androgen receptor and RNase L mediates a cross-talk between the interferon and androgen signaling pathways. *J. Biol. Chem.*, **280**, 38898–38901.
51. Basrawala, Z., Alimirah, F., Xin, H., Mohideen, N., Campbell, S., Flanagan, R. and Choubey, D. (2006) Androgen receptor levels are increased by interferons in human prostate stromal and epithelial cells. *Oncogene*, **25**, 2812–2817.
52. Lin, B., Ferguson, C., White, J., Wang, S., Vessella, R., True, L., Hood, L. and Nelson, P.S. (1999) Prostate-localized and androgen-regulated expression of the membrane-bound serine protease TMPRSS2. *Cancer Res.*, **17**, 4180–4184.
53. Huang, Q., Li, W., Zhou, Q., Awasthi, P., Cazin, C., Yap, Y., Mladenovic-Lucas, L., Hu, B., Jeyasuria, P., Zhang, L. et al. (2021) Leucine zipper transcription factor-like 1 (LZTFL1), an intraflagellar transporter protein 27 (IFT27) associated protein, is required for normal sperm function and male fertility. *Dev. Biol.*, **477**, 164–176.
54. Baldassarri, M., Picchiotti, N., Fava, F., Fallerini, C., Benetti, E., Daga, S., Valentino, F., Doddato, G., Furini, S., Giliberti, A. et al. (2021) Shorter androgen receptor polyQ alleles protect against life-threatening COVID-19 disease in European males. *EBioMedicine*, **65**, 103246. <https://doi.org/10.1016/j.ebiom.2021.103246>.
55. Harris, P., Taylor, R., Thielke, R., Payne, J., Gonzalez, N. and Conde, J. (2009) Research electronic data capture (REDCap)—a metadata-driven methodology and workflow process for providing translational research informatics support. *J. Biomed. Inform.*, **42**, 377–381.
56. Harris, P., Taylor, R., Minor, B., Elliott, V., Fernandez, M., O'Neal, L., McLeod, L., Delacqua, G., Delacqua, F., Kirby, J. et al. (2019) The REDCap consortium: building an international community of software partners. *J. Biomed. Inform.*, **95**, 103208. <https://doi.org/10.1016/j.jbi.2019.103208>.
57. The 1000 Genomes Project Consortium (2015) A global reference for human genetic variation. *Nature*, **526**, 68–74.
58. Purcell, S., Ben, N., Todd-Brown, K., Thomas, L., Ferreira, M., Bender, D., Maller, J., Sklar, P., de Bakker, P., Daly, M. et al. (2007) PLINK: a tool set for whole-genome association and population-based linkage analyses. *Am. J. Hum. Genet.*, **81**, 559–575.
59. Graffelman, J. and Moreno, V. (2013) The mid P-value in exact tests for hardy-Weinberg equilibrium. *Stat. Appl. Genet. Mol. Biol.*, **12**, 433–448.
60. Price, A., Weale, M., Patterson, N., Myers, S., Need, A., Shianna, K., Ge, D., Rotter, J., Torres, E., Taylor, Q. et al. (2008) Long-range LD can confound genome scans in admixed populations. *Am. J. Hum. Genet.*, **83**, 132–139.
61. Alexander, D., Novembre, J. and Lange, K. (2009) Fast model-based estimation of ancestry in unrelated individuals. *Genome Res.*, **19**, 1655–1664.
62. Taliun, D., Harris, D., Kessler, M., Carlson, J., Szpiech, Z., Torres, R., Galiano Taliun, S., Corvelo, A., Gogarten, S., Kang, H. et al. (2021) Sequencing of 53,831 diverse genomes from the NHLBI TOPMed program. *Nature*, **590**, 290–299.
63. Zheng, X., Levine, D., Shen, J., Gogarten, S., Laurie, C. and Weir, B. (2012) A high-performance computing toolset for relatedness and principal component analysis of SNP data. *Bioinformatics*, **28**, 3326–3328.
64. Zheng, X. and Davis, W. (2021) SAIGEgds—an efficient statistical tool for large-scale PheWAS with mixed models. *Bioinformatics*, **37**, 728–730.
65. Zhou, W., Nielsen, J., Fritsche, L., Dey, R., Gabrielsen, M., Wolford, B., LeFaive, J., VandeHaar, P., Gagliano, S., Figgord, A. et al. (2018) Efficiently controlling for case-control imbalance and sample relatedness in large-scale genetic association studies. *Nat. Genet.*, **50**, 1335–1341.
66. Willer, C., Li, Y. and Abecasis, G. (2010) METAL: fast and efficient meta-analysis of genomewide association scans. *Bioinformatics*, **26**, 2190–2191.
67. Hutchinson, A., Watson, H. and Wallace, C. (2020) Improving the coverage of credible sets in Bayesian genetic fine-mapping. *PLoS Comput. Biol.*, **16**, e1007829. <https://doi.org/10.1371/journal.pcbi.1007829>.
68. Yang, J., Lee, H., Goddard, E. and Visscher, P. (2011) GCTA: a tool for genome-wide complex trait analysis. *Am. J. Hum. Genet.*, **88**, 76–82.
69. Templeton, A. and Read, B. (1994) Inbreeding: one word, several meanings, much confusion. *EXS*, **68**, 91–105.